Zeitschrift für Kristallographie, Bd. 109, S. 161—183 (1957)

The Crystal Structure of Jamesonite, $FePb_4Sb_6S_{14}$

By N. NIIZEKI[1] and M. J. BUERGER

With 19 figures

(Received February 25, 1957)

Zusammenfassung

Die Kristallstruktur des Jamesonits gehört der Raumgruppe $P2_1/a$ an; die Elementarzelle mit den Gitterkonstanten $a = 15{,}07$ Å, $b = 18{,}98$ Å, $c = 4{,}03$ Å, $\beta = 91°48'$ enthält 2 $FePb_4Sb_6S_{14}$.

Drei SbS_3-Gruppen sind parallel [120] angeordnet und können zusammen als Sb_3S_7-Gruppen aufgefaßt werden, die durch lose Bindung größere Gruppen Sb_6S_{14} ergeben. Fe- und zwei Lagen von Pb-Atomen nehmen die Räume zwischen S-Atomen der Sb_6S_{14}-Gruppen ein und verknüpfen die Sb-S-Gruppen miteinander. Jedes Fe-Atom wird von sechs S-Atomen in den Ecken eines verzerrten Oktaeders umgeben. Die Pb-Atome haben entweder 7 oder 8 S-Atome als nächste Nachbarn. Starke Bindung längs Ketten oder Schichten parallel der Längsrichtung der nadeligen Kristalle tritt beim Jamesonit nicht klar in Erscheinung. Die Spaltbarkeit des Minerals wird auf Grund der beobachteten interatomaren Abstände gedeutet.

Abstract

The crystal structure of the mineral jamesonite has been determined. The space group is $P2_1/a$, and the unit cell dimensions are: $a = 15.07$ Å, $b = 18.98$ Å, $c = 4.03$ Å, and $\beta = 91°48'$. This unit cell contains 2 $FePb_4Sb_6S_{14}$. The intensities were measured by the single-crystal GEIGER-counter method with Cu$K\alpha$ radiation. The structure projected along c axis was solved by the minimum function method. The z parameters of the atoms were determined by the implication method. The structure was refined by the successive FOURIER, and difference-FOURIER trials, and finally by the three-dimensional least-squares method.

In the structure three SbS_3 groups are arranged parallel to [120], and can be described as forming Sb_3S_7 groups. Two Sb_3S_7 groups are loosely bonded together into a larger Sb_6S_{14} group. Fe and two kinds of Pb atoms are located in the interstices provided by the S atoms of the Sb_6S_{14} groups, and play the role of cementing these Sb-S groups. Fe has a distorted octahedral coordination of six S atoms. The Pb atoms have either 7 or 8 atoms of sulfur as closest neighbors.

[1] Present address: Mineralogical Institute, University of Tokyo, Tokyo, Japan.

The strongly bonded chains or layers running parallel to the acicular axis of the mineral is not well defined in jamesonite. The cleavage of the mineral has been accounted for in terms of the observed interatomic distances.

Introduction

The crystallographic description of the mineral jamesonite, $FePb_4Sb_6S_{14}$, has been presented by BERRY[2]. Jamesonite is a member of the group of acicular sulfosalts, concerning which there has been a considerable increase in structural knowledge in recent years[3–7]. As in the case of livingstonite[6], $HgSb_4S_8$, the crystal system of jamesonite is monoclinic. The needle axis of jamesonite is parallel to the c axis, while in livingstonite it is parallel to the unique 2-fold (or b) axis.

The cleavages of the members of the group of acicular sulfosalts are known to occur in two ways. In one type, cleavage parallel to the acicular axis, or prismatic cleavage only, is observed. All the sulfosalts crystals of the acicular group with previously determined structures are of this type. In these crystal structures there are layers or chains composed of submetal atoms and sulfur atoms running parallel to the needle axis of the mineral. The prismatic cleavage of the mineral has been explained as due to the breaking of the weaker chemical bonds between the layers or chains in the structure, and, as a result, parallel to the acicular axis. A second type of cleavage occurs perpendicularly to the acicular axis. This basal cleavage is observed with or without accompanying prismatic cleavage. Among the minerals with this type of cleavage are jamesonite, owyheeite[8], and falkmanite[9]. Accordingly, a somewhat different structural scheme than found in the previously determined structures can be expected for jamesonite.

[2] L. G. BERRY, Studies of mineral sulpho-salts: II. Jamesonite from Cornwall and Bolivia. Miner. Mag. **25** (1940) 597—608.

[3] F. E. WICKMAN, The crystal structure of galenobismutite. Arkiv Chem. Geol. **1** (1951) 219—225.

[4] F. E. WICKMAN, The crystal structure of aikinite, $CuPbBiS_3$. Arkiv Chem. Geol. **1** (1953) 501—507.

[5] M. J. BUERGER and THEODOR HAHN, The crystal structure of berthierite, $FeSb_2S_4$. Am. Mineralogist **40** (1955) 226—238.

[6] N. NIIZEKI and M. J. BUERGER, The crystal structure of livingstonite, $HgSb_4S_8$. Z. Kristallogr. **109** (1957) 129—157.

[7] N. NIIZEKI, The crystal chemistry of the mineral sulfosalts. To be published in Geochemica Acta.

[8] S. C. ROBINSON, Owyheeite. Am. Mineralogist **34** (1949) 398—402.

[9] J. E. HILLER, Über den Falkmanit und seine Unterscheidung von Boulangerit. Neues Jb. Mineralog. Mh. **1955**, 1—10.

Unit cell and space group

The unit cell and space group of the mineral were determined from precession and DE JONG photographs using crystals from Cornwall, England, kindly furnished for our investigation by Professor CLIFFORD FRONDEL from the Harvard mineralogical collection. The results obtained for the unit cell dimensions are:

$$a = 15.57 \text{ Å}$$
$$b = 18.98 \text{ Å} \qquad \beta = 91°48'$$
$$c = 4.03 \text{ Å}$$

These values are in good agreement with those of BERRY. The space group $P2_1/a$ assigned by BERRY[2] was confirmed. The unit cell contains $2FePb_4Sb_6S_{14}$.

Intensity determination

A single crystal of needle form having dimensions 0.03 mm. × 0.04 mm. × 1.5 mm. was selected for the intensity determination. The three-dimensional intensities were measured by the single-crystal

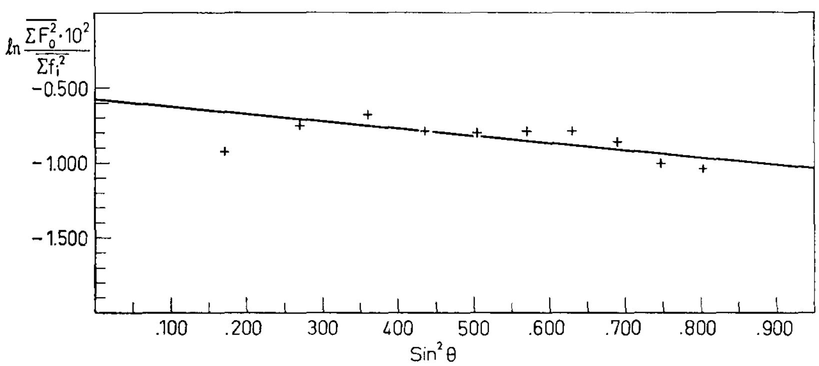

Fig. 1. Determination of scale factor and temperature coefficient by WILSON's statistical method applied to three-dimensional intensity data

GEIGER-counter goniometer method developed in the Crystallographic Laboratory, M.I.T., using Cu$K\alpha$ radiation. Intensities were corrected for LORENTZ and polarization factors, but no allowance was made for the absorption factor. The $F^2(hkl)$ values were placed on an absolute basis using WILSON's method[10] applied three-dimensionally, Fig. 1. The temperature coefficient obtained by this method was $B = 0.59$.

[10] A. J. C. WILSON, Determination of absolute from relative intensity data. Nature **150** (1942) 151—152.

General outline of the structure determination

Space-group equipoint considerations fix the position of the Fe atoms on one set of centers of symmetry. All the rest of the atoms presumably must occupy the general position $4(e)$. The existence of one short axis of length 4 Å suggests the possibility of solving the crystal structure as projected along this axis by means of minimum function method[11].

As pointed out by BUERGER and HAHN elsewhere[5], errors in solutions by the minimum-function method can arise if the PATTERSON peak chosen as the image point is not a single peak, but rather a coalescence of several peaks. During the present case of the structure determination of jamesonite, a false structure was obtained from an image point incorrectly selected. This false structure appeared very similar to the expected structure, at least in numbers of heavy peaks representing Pb and Sb atoms. The falseness of the structure could not be detected until a final electron-density map indicated certain abnormalities of the structure. Since this kind of confusion is apt to occur when the image-seeking method is applied to solve structures with large unit cells having many heavy atoms, such as those of many of the sulfosalt minerals, the discussion of the procedure will be given in some detail.

Interpretation of PATTERSON peaks

The PATTERSON map $P(xy)$, Fig. 2, was obtained from the $F^2(hk0)$'s. The plane group of the projection along the c axis of space group $P2_1/a$ is $p2gg$, and the corresponding PATTERSON plane group is $p2mm$. The relation between a rotation peak and its reflection satellites in this plane group is illustrated in Fig. 3. Since there are 2 Pb atoms and 3 Sb atoms in the asymmetric unit, then if no overlapping occurs, there must be 5 rotation peaks of single weight, and 10 reflection satellites of double weight in a quarter of PATTERSON space. Actually, as shown in Fig. 2, there are 6 peaks along the line $x = {}^1/_2$, and 8 peaks along the line $y = {}^1/_2$. These peaks have various heights, and the broadened shapes of some peaks at once suggest a considerable amount of overlapping at these locations. The excess number of peaks appearing along these lines is considered due either to interatomic vectors with accidental x or y component of ${}^1/_2$, or coalescence of reflection satellites of S atoms.

---

[11] M. J. BUERGER, A new approach to crystal-structure analysis. Acta Crystallogr. 4 (1951) 531–544.

Since it was impossible to choose definite satellite peaks, all the satellite-like peaks were used to find possible rotation peaks. Among the 48 possible positions for rotation peaks, Fig. 4, only three of them are associated with peaks which can be assumed reasonably as single-weight rotation peaks. The peak-height analysis was made assuming

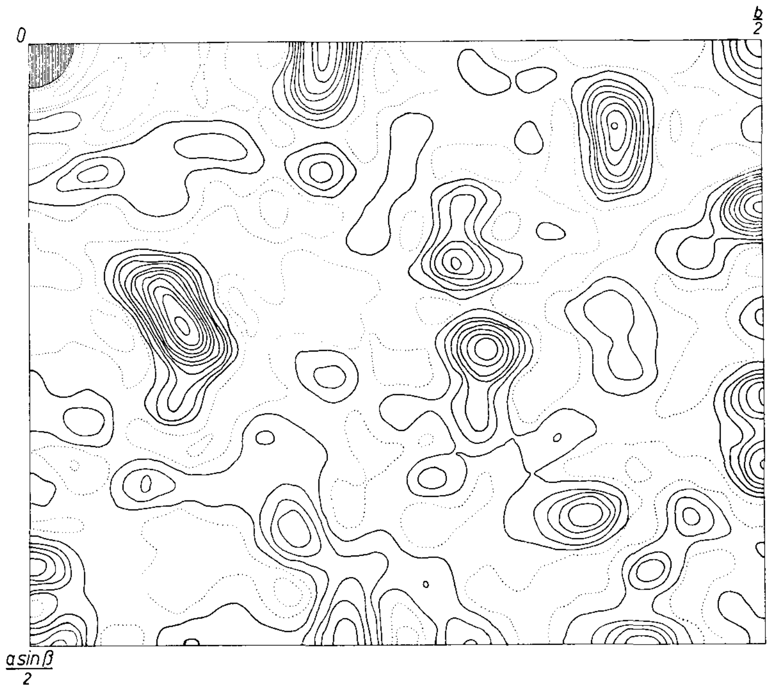

Fig. 2. PATTERSON diagram $P(xy)$. Contours are drawn at intervals of 50 units on an arbitrary scale. The dotted contours represent depressions. The details of the heavy peak at the origin are omitted.

a probably true zero contour, and it was found that all three of the peaks could be Pb—Pb rotation peaks. These peaks are numbered I, II, and III in Fig. 4.

Solutions by the image-seeking method

Assuming each of these three peaks as an image point in turn, three sets of M_2 functions were obtained, and each of them was folded into an M_4 function using a glide operation. These three M_4 maps are shown in Figs. 5, 6 and 7. Among them the ${}^{III}M_4$ map (an M_4 map based upon the assumption that peak III is a Pb—Pb rotation peak) gave a result completely unrelated to the expected number of heavy atoms in the structure, Fig. 7, and was accordingly discarded. Since both the ${}^{I}M_4$ map and the ${}^{II}M_4$ map gave 6 heavy peaks, no choice between them was considered at this stage. The structures based on peaks I and II will be identified as structures I and II, respectively. To resolve an extra peak in each map ,another M_4 map was tried for each structure. The peak with the heaviest contour in each M_4 map was assumed as the second probable atomic site for the *Pb* atom. In structure I, Fig. 5, it is designated as peak *a*, and in structure II, Fig. 6, as peak *A*. The ${}^{a}M_4$ map and the ${}^{A}M_4$ map were then prepared. Under the assumption that the atoms at I and *a* in one structure, and II and *A* in the other, are all of the same atomic specie (i. e., *Pb*) the ${}^{I+a}M_8$ and ${}^{II+A}M_8$ maps can be obtained by superposing the proper M_4 maps. The ${}^{I+a}M_8$ map, which was later found to represent the correct structure, is shown in Fig. 8. Also in Fig. 9, two M_8 maps were compared, one map ${}^{I+a}M_8$ in full lines, and the other ${}^{II+A}M_8$ in dotted lines. From this comparison, however, nothing indicates which is the correct one.

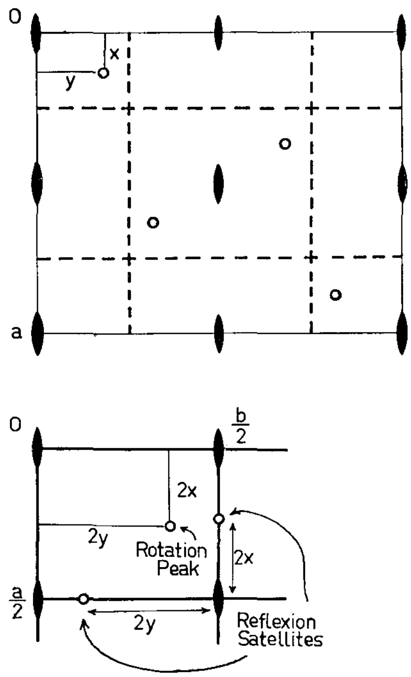

Fig. 3. Geometrical relation between a rotation peak and its reflection satellites in Patterson diagrams having plane symmetry $p2mm$

False structure

First the structure II was assumed to be correct, and since the identification of heavy peaks in the M_8 map with Pb and Sb was impossible, structure factors were computed using an average f curve: $^1/_2\,(f_{\text{Pb}} + f_{\text{Sb}})$. An electron-density map was prepared using signs determined in this way, and then refined by the usual procedures. The final electron-density map of structure II and its structural scheme, are shown respectively in Figs. 10 and 11. An examination of $\varrho(xy)$, Fig. 10, however, reveals several peculiarities which are enough to raise a question as to the validity of this structure. First, the relative weights of the five heavy peaks do not correspond to the chemical formula of jamesonite in a clear-cut way. Above all, there is one peak (peak *D* in Fig. 10) significantly too low to be assigned to an Sb atom. Furthermore, the shape of this particular peak is not well defined. The

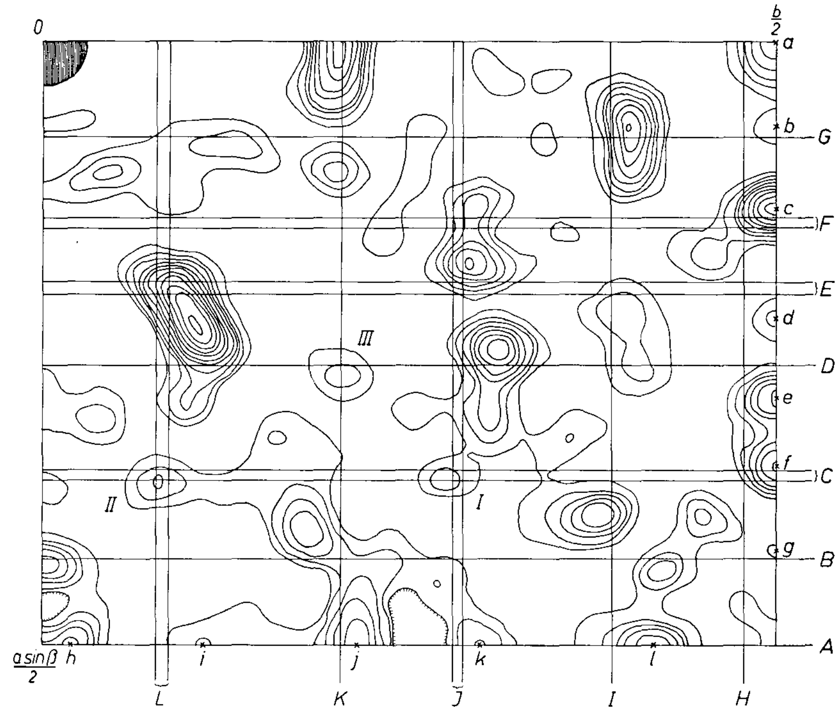

Fig. 4. Solution of rotation peaks from satellite-like peaks. Solutions are obtained at the intersections of horizontal and vertical lines drawn according to the relation illustrated in Fig. 3. Satellite-like peaks are designated by letters *a* to *l*, and the corresponding lines are designated by letters *A* to *L*. Three probable rotation peaks obtained by this method are indicated by I, II, and III.

above-mentioned aspects of the structure could not be improved by exchanging Pb with Sb in some of the atomic sites. Second, the peak shapes of the lighter atoms, especially of the Fe atom at the origin, are obscure. For these reasons structure II was considered incorrect. The significance of those features in the FOURIER diagrams which suggest an incorrect structure was recently pointed out by PINNOCK et al.[12].

[12] P. R. PINNOCK, C. A. TAYLOR and H. LIPSON, A re-determination of the structure of triphenylene. Acta Crystallogr. 9 (1956) 173–179.

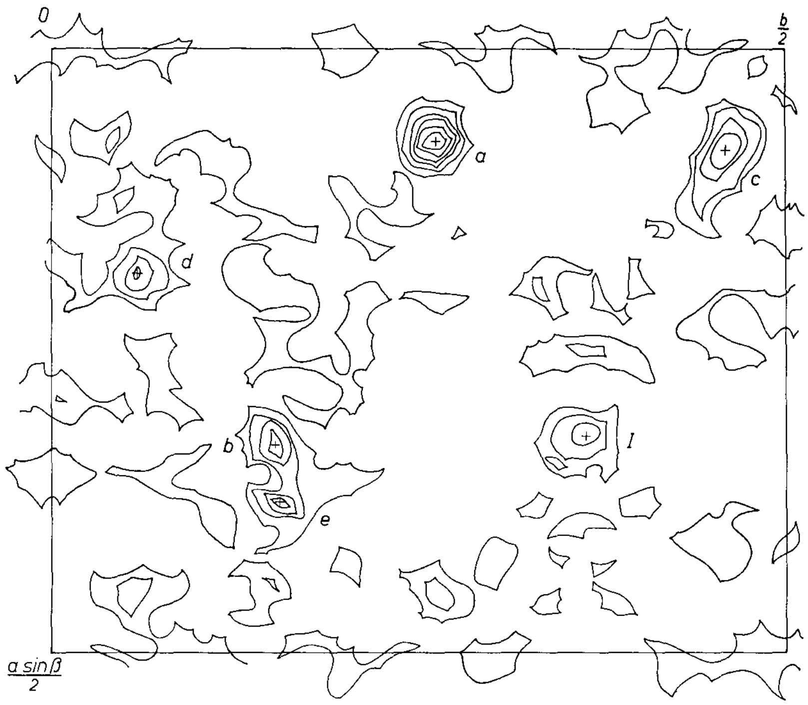

Fig. 5. $^{I}M_4$ map

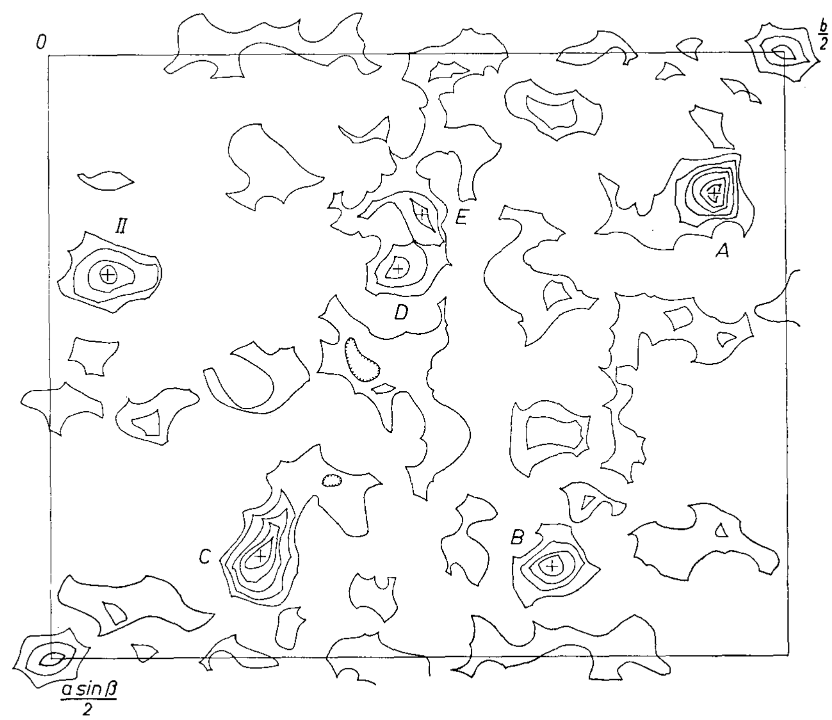

Fig. 6. $^{II}M_4$ map

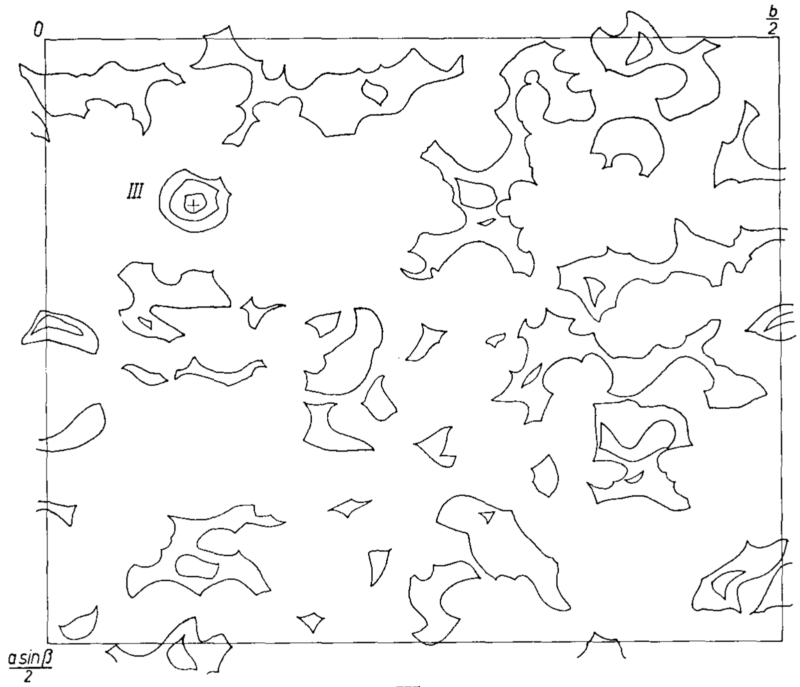

Fig. 7. $^{III}M_4$ map

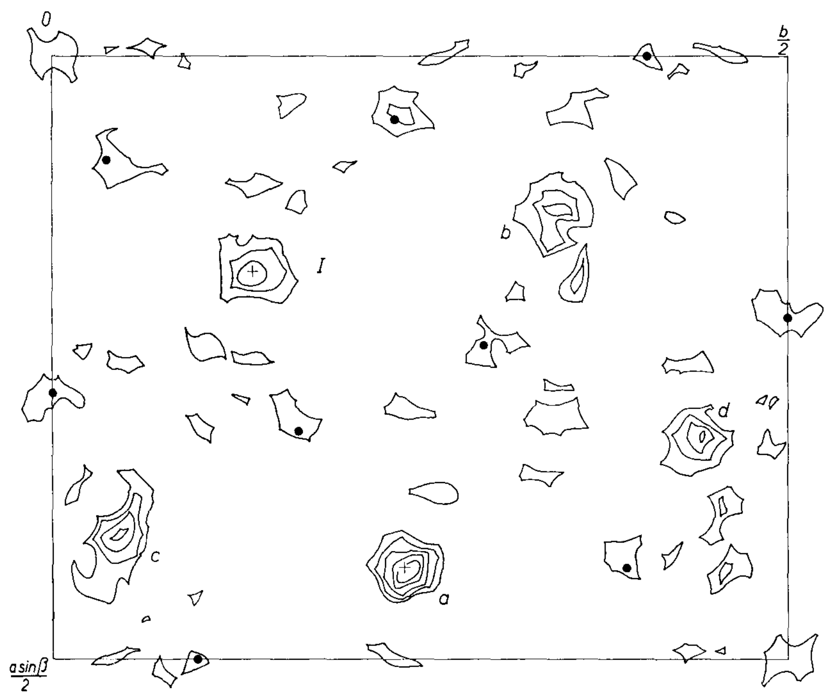

Fig. 8. $^{I+a}M_8$ map. Black dots indicate the final atomic sites for S atoms determined by FOURIER methods

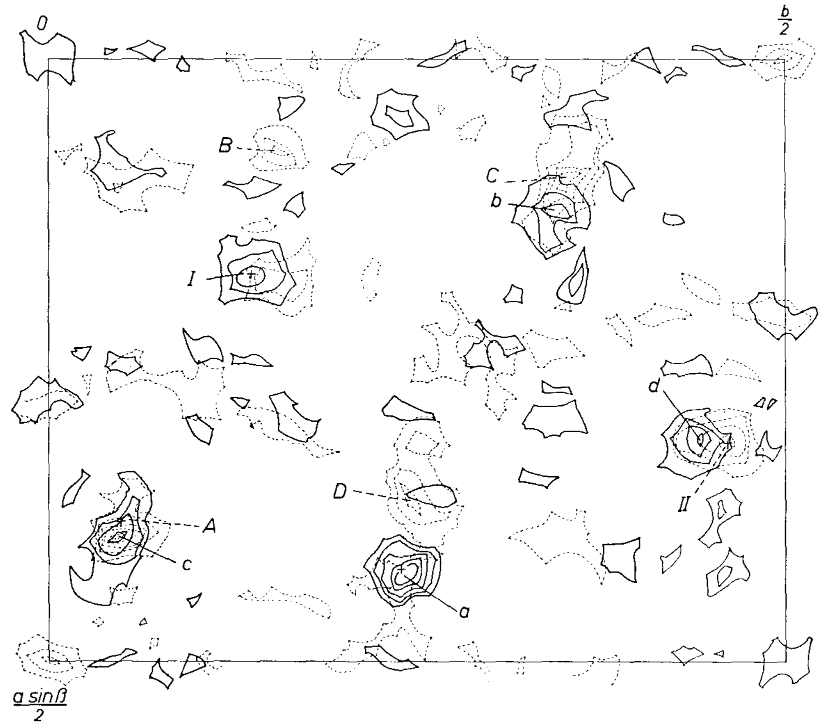

Fig. 9. Comparison of two M_8 maps. The $^{I+a}M_8$ map is drawn in full lines, and the $^{II+A}M_8$ map in broken lines

Correct structure

The alternative structure I based on the $^{I+a}M_4$ map was then tried. Structure factors were computed as before with the averaged f curve. The electron-density map is shown in Fig. 12. In this map the shapes and the weight relations among the five heavy peaks are well defined. Peaks I and a are assigned to Pb atoms, and peaks b, c, and d to the three Sb atoms.

Because of the identity of peaks I and a, the superposition of the $^{I}M_4$ map and the $^{a}M_4$ map was justified, and this $^{I+a}M_8$ map, Fig. 8, should contain enough information concerning the locations of S atoms. Although the refinement of the electron-density map, Fig. 12, should naturally indicate the sulfur peaks, it was considered useful to see how the image-seeking method would narrow the allowed region for the S atoms. This process was carried out by further constructing a $^{b+c}M_8$ map based on the rotation peaks b and c, both Sb—Sb rotation peaks. This map is shown in broken lines in Fig. 13 superposed on the previously obtained ${}^{I+a}M_8$ map, which is drawn in full lines. Since these two M_8 maps are based on rotation peaks of different weights (different atomic species), the simple superposition to obtain an M_{16} map could not be made without proper weighting of contours. The final sulfur positions found by the FOURIER method are indicated in

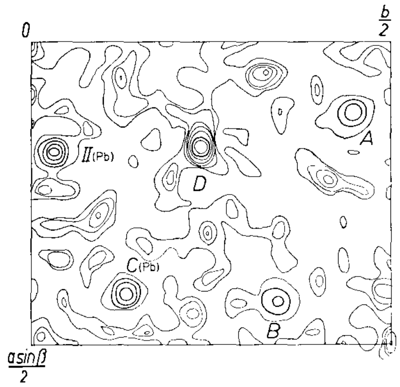

Fig. 10

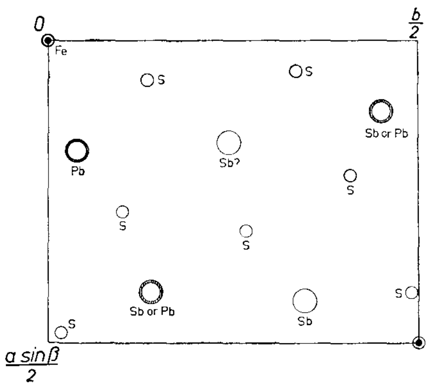

Fig. 11

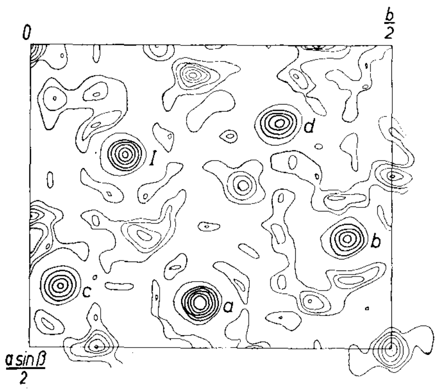

Fig. 12

Fig. 10. Electron density map $\varrho(xy)$ of false structure based on ${}^{II+A}M_8$ map

Fig. 11. Structural scheme of false structure, Fig. 10

Fig. 12. Electron density map $\varrho(xy)$ of correct structure based on ${}^{I+a}M_8$ map

Fig. 13 by black dots. They are all found at locations permitted by the minimum-function maps. Including these sulfur atoms in the structure-factor computation, the refinement of structure I was done by successive difference-FOURIER maps. The final atomic coordinates determined by this process are presented in Column III of Table 1. The reliability factor for this projection was computed as $R = 0.19$.

The final electron density map prepared with signs after the three-dimensional refinement is shown in Fig. 14 for the full unit cell.

Table 1. *Atomic coordinates determined by several methods*

Atom	I From minimum-function map		II From implication-map	III From Fourier maps		
	x	y	z	x	y	z
Pb_{I}	0.183	0.136	0.060	0.184	0.139	0.066
Pb_{II}	0.425	0.240	0.060	0.428	0.240	0.040
Sb_{I}	0.320	0.436	0.480	0.320	0.436	0.488
Sb_{II}	0.400	0.050	0.570	0.398	0.049	0.592
Sb_{III}	0.128	0.346	0.620	0.132	0.340	0.628
S_{I}				0.423	0.393	0.000
S_{II}				0.102	0.043	0.460
S_{III}				0.316	0.160	0.540
S_{IV}				0.227	0.296	0.940
S_{V}				0.045	0.230	0.560
S_{VI}				0.010	0.397	0.920
S_{VII}				0.282	0.009	0.060
Fe				0.000	0.000	0.000
				$R(hk0) = 0.19$ $R(h0l) = 0.24$ $R(hkl) = 0.28$		

Determination of z coordinates of atoms

The z parameters of the heavy atoms were determined by the implication method[13]. A Harker synthesis $P(x\,\frac{1}{2}\,z)$ was performed and the result is shown in Fig. 15. The relations between crystal space, Patterson space, and implication space are illustrated in Fig. 16 for the general equipoints $2(e)$ of plane group $p2$. There are sub-multiple translations of $a/2$ in these projections. In Fig. 17, therefore, the implication map corresponding to this sub-multiple cell is shown. Underneath the $I(x\,\frac{1}{2}\,z)$ map is placed the heavy atoms with the x coordinates determined from $\varrho(xy)$. The 4-fold ambiguities were resolved first by assuming as zero the z coordinate of the center of symmetry where the Fe atom is located, then by measuring the projected interatomic distances in $\varrho(xy)$. Approximate z coordinates for the Pb atom were found to be zero, and those for Sb atoms were found to be $c/2$. The z parameters determined in this way are tabulated in Column II of Table 1. A few extra peaks of medium weights are observed in the

[13] M. J. Buerger, The interpretation of Harker syntheses. J. Appl. Physics **17** (1946) 579—595.

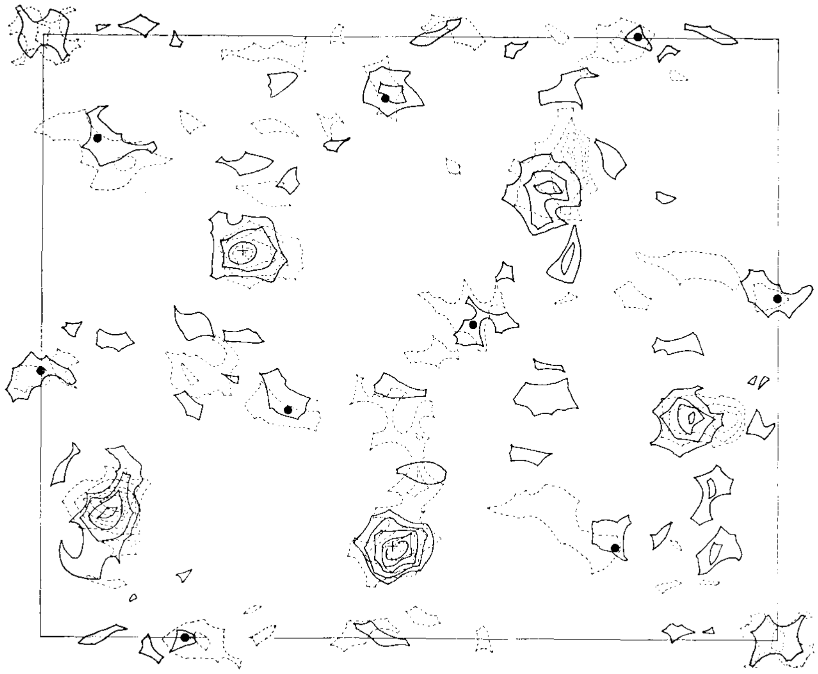

Fig. 13. Two M_8 maps superposed. The ${}^{1+a}M_8$ map is drawn in full lines, and the ${}^{b+c}M_8$ map in dotted lines. Black dots indicate the final locations of S atoms determined by FOURIER methods.

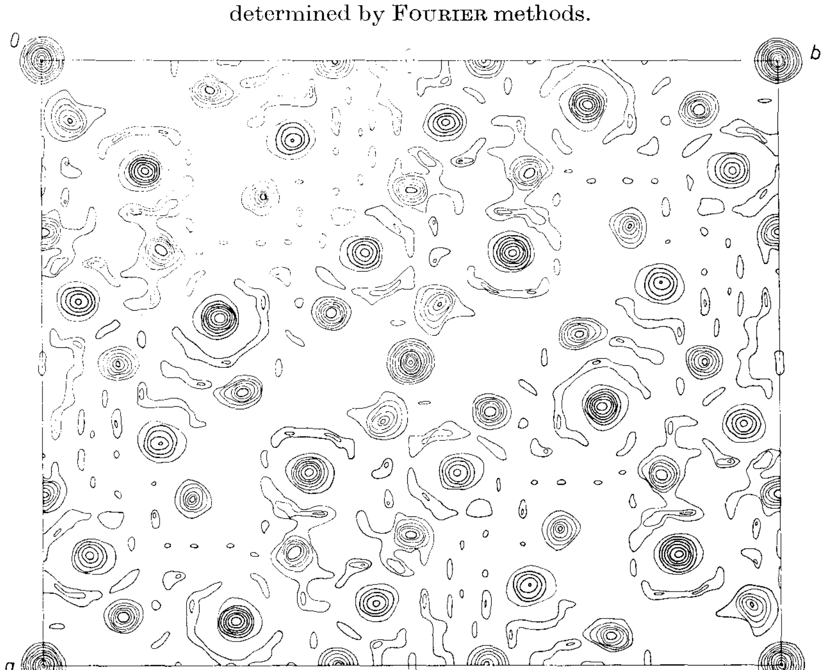

Fig. 14. Final electron density map $\varrho(xy)$

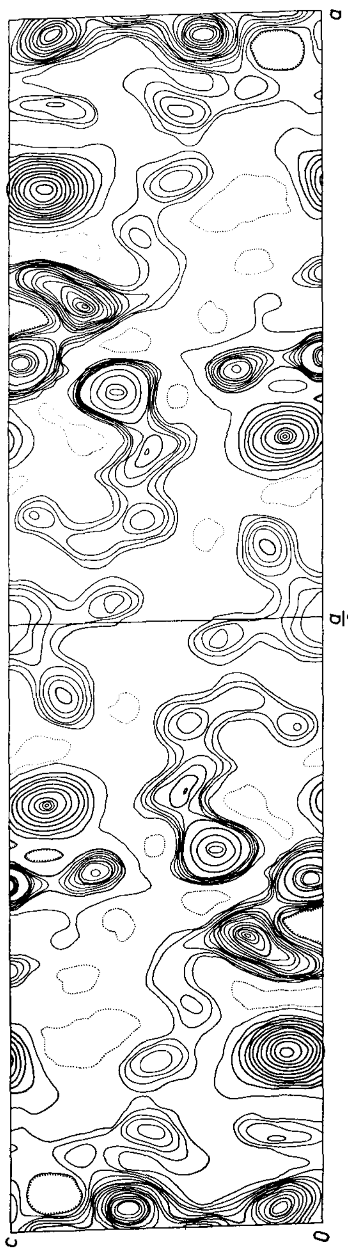

Fig. 15. HARKER section $P(x\frac{1}{2}z)$. Heavy contours represent the intervals of five light contours. The details between the heavy contours are omitted

implication map, Fig. 17. These are explained as due to interatomic vectors between atoms not related by a screw operation, but with y components of nearly $^1/_2$. Such a vector gives part of a PATTERSON peak in a HARKER section.

With an initial set of signs of structure factors determined by the heavy atoms, an electron-density map $\varrho(xz)$ was obtained, and then refined in the usual way. The final z coordinates determined by the FOURIER method are tabulated in Column III of Table 1, along with x and y coordinates. The reliability factor of this projection was computed as $R = 0.24$. This value was considered as low enough to proceed to three-dimensional refinement. The electron-density map $\varrho(xz)$ of the final structure is shown in Fig. 18.

Three-dimensional refinements

The three-dimensional refinement of the structure was performed by the least-squares method developed by SAYRE[14] at the International Business Machine Corp., New York. The initial reliability factor of 1100 $F(hkl)$'s was $R = 0.28$. After six cycles of the refinement process it went down to $R = 0.166$. Since no allowance was made for the

[14] P. H. FRIEDLANDER, W. LOVE and D. SAYRE, Least-squares refinement at high speed. Acta Crystallogr. 8 (1955) 732.

absorption effect, this value was regarded as sufficiently low to assure the accuracy of the structure.

The final atomic coordinates are tabulated in Table 2. The comparison between observed and computed structure factors is given in Table 4.

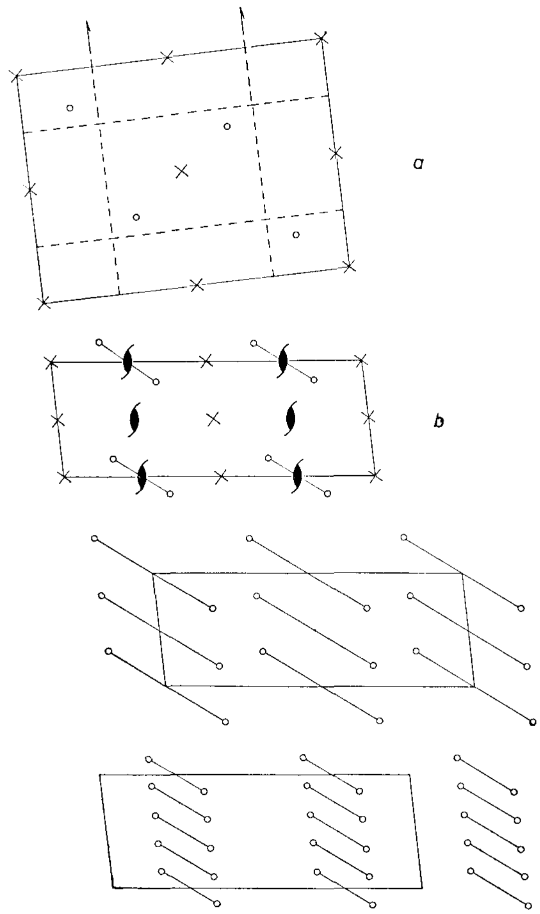

Fig. 16. Relations between crystal space, PATTERSON space, and implication space. In drawings (*a*) and (*b*), space group $P2_1/a$ is shown in two projections. In crystal space the general equipoints 4(*e*) are indicated by small circles. Drawing (*c*) represents the HARKER section derived from (*b*). The origin is shifted from a center of symmetry to a 2_1 axis. The submultiple translation $a/2$ is evident. In drawing (*d*) is shown the corresponding implication space, $I(x\frac{1}{2}z)$. The origin is again shifted to a center of symmetry to compare with the crystal space. The 4-fold ambiguity is evident.

Discussion of the structure

The interatomic distances between neighboring atoms are tabulated in Table 3. These distances are also indicated in a diagrammatic representation of the structure, Fig. 19.

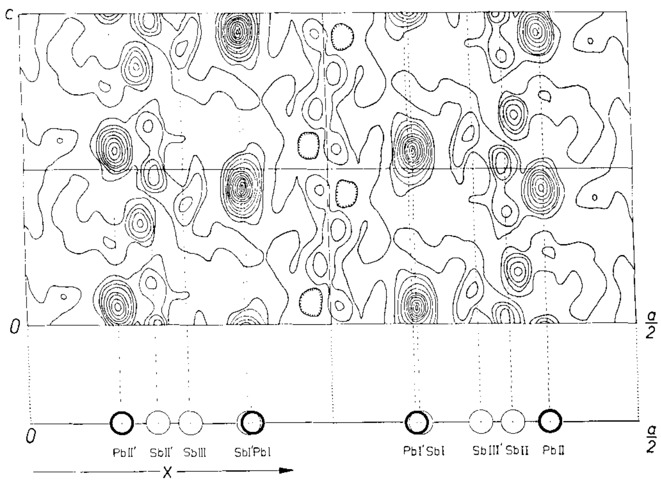

Fig. 17. Implication map $I(x\frac{1}{2}z)$, and its interpretation. In the upper drawing the implication map is shown. In the lower drawing the x coordinates of the heavy atoms are indicated by circles on the straight line. The atoms related to each other by screw operations are indicated by primes. The z coordinate of each atom can be determined by tracing up the broken line into the implication map. Two-fold ambiguity of the solution is solved if interatomic distances in the projection $\varrho(xy)$, Fig. 14, are taken into consideration.

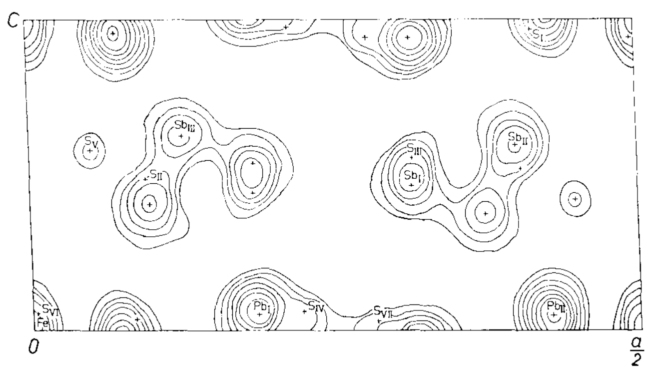

Fig. 18. Final electron density map $\varrho(xz)$

Table 2. *Final coordinates and temperature coefficients of atoms in jamesonite*

Atom	x	y	z	B
Pb_I	0.182	0.141	0.036	1.21
Pb_{II}	0.425	0.240	0.062	1.08
Sb_I	0.319	0.437	0.408	0.75
Sb_{II}	0.396	0.049	0.623	0.74
Sb_{III}	0.130	0.340	0.620	1.05
S_I	0.419	0.395	0.968	0.21
S_{II}	0.095	0.042	0.524	0.59
S_{III}	0.316	0.158	0.555	0.73
S_{IV}	0.226	0.297	0.076	0.73
S_V	0.050	0.230	0.573	0.17
S_{VI}	0.002	0.398	0.052	0.71
S_{VII}	0.285	0.004	0.027	0.41
Fe	0.000	0.000	0.000	1.08

Note: $R = 0.166$ for 1100 $F(hkl)$'s with this structure. B values were determined in the processes of three-dimensional least-squares refinement.

Table 3. *Interatomic distances in jamesonite*

	S_I	S_{II}	S_{III}	S_{IV}	S_V	S_{VI}	S_{VII}
Pb_I		3.01 Å 3.13	2.91 Å 2.92	3.04 Å	3.29 Å		3.04 Å
Pb_{II}	2.97 Å		3.04 3.08	3.28	2.85 2.87	2.88 Å	
Sb_I	2.52 2.82	2.41				3.29 4.08	2.67 2.90
Sb_{II}			2.43			2.56 3.04 3.51 4.29	2.56 3.07
Sb_{III}				2.56 2.81	2.44	3.18 2.94	3.67 4.40
Fe	2.36 (2)	2.57 (2) 2.66 (2)					

If account is taken of the nearest neighbors only, each of the three kinds of Sb atoms has three S atoms at distances of about 2.5 Å. The Sb and S atoms thus form an SbS_3 group of trigonal-pyramidal shape. But this SbS_3 group, described in terms of the three shortest distances, is different in its orientation from the corresponding groups found in previously determined structures. In the structures of other sulfosalts, one edge of the pyramid is found to be parallel to the 4 Å axis. In jamesonite none of the edges is oriented in this way, but one edge is found as approximately parallel to the (001) plane.

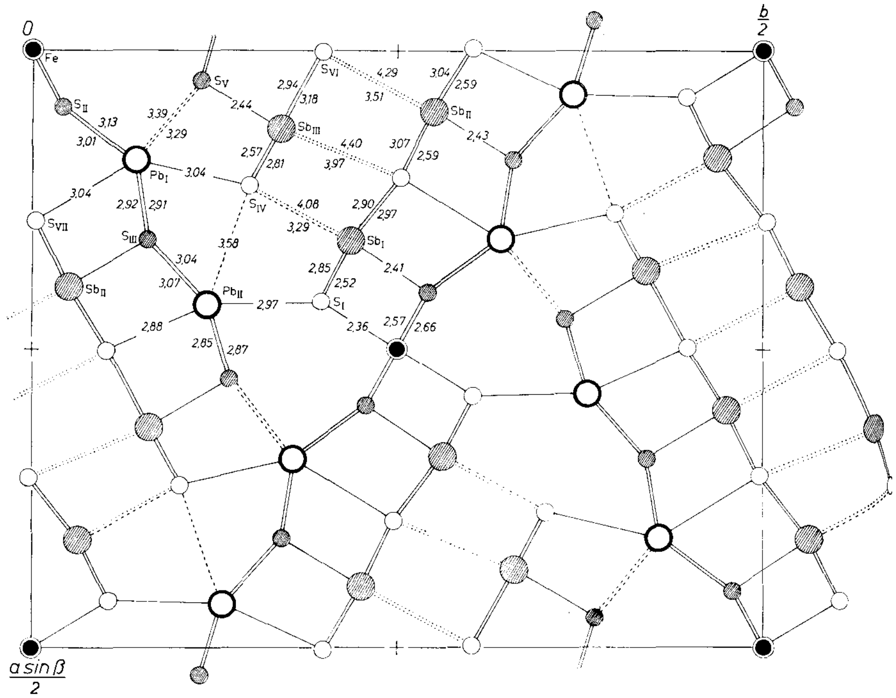

Fig. 19. Schematic representation of the structure. Open circles represent atoms with z coordinates close to zero, and shaded circles represent atoms with z coordinates close to $\frac{1}{2}$. The chemical bonds between neighboring atoms are indicated by lines. Broken lines are used to show the additional bonds from Pb to S beside the distorted octahedral bonds. Dotted lines indicate the weak bonds between Sb and S. All figures showing interatomic distances are in Å units.

Three such groups, $Sb_{(I)}S_3$, $Sb_{(II)}S_3$, and $Sb_{(III)}S_3$ are arranged in an almost straight line parallel to [120]. Each trigonal pyramid shares corners with neighboring pyramids and forms an Sb_3S_7 group. The distance between Sb atoms in the group and S atoms in their translation-equivalent group along the c axis is about 3.0 Å, and there is no strongly bonded Sb—S layer running parallel to the 4 Å axis in jamesonite.

Table 4. *Observed and calculated structure factors*

h k l	$\|F_{obs}\|$	F_{calc}	h k l	$\|F_{obs}\|$	F_{calc}	h k l	$\|F_{obs}\|$	F_{calc}	h k l	$\|F_{obs}\|$	F_{calc}	h k l	$\|F_{obs}\|$	F_{calc}
0 2 0	97	- 101	4 7 0	259	- 270	8 8 0	240	- 228	13.10.0	51	- 31	2 6 $\bar{1}$	259	- 248
0 4 0	63	+ 20	4 8 0	142	+ 113	8 9 0	249	- 220	13.11.0	179	+ 163	2 7 $\bar{1}$	340	- 316
0 6 0	151	- 70	4 9 0	369	+ 406	8.10.0	287	+ 268	13.12.0	101	+ 102	2 8 $\bar{1}$	71	- 60
0 8 0	206	+ 182	4.10.0	414	+ 433	8.11.0	133	+ 116	14.0.0	115	- 93	2 9 $\bar{1}$	95	+ 58
0.10.0	585	- 630	4.11.0	50	- 62	8.12.0	39	- 19	14.1.0	187	+ 159	2.10.$\bar{1}$	79	+ 56
0.12.0	158	+ 107	4.13.0	53	+ 12	8.13.0	82	- 50	14.2.0	268	- 210	2.11.$\bar{1}$	28	- 21
0.14.0	118	+ 116	4.14.0	94	+ 86	8.14.0	136	- 136	14.3.0	46	- 30	2.13.$\bar{1}$	458	+ 506
0.16.0	105	+ 71	4.15.0	55	- 23	8.15.0	94	+ 75	14.4.0	278	+ 238	2.14.$\bar{1}$	194	- 173
0.18.0	127	+ 80	4.16.0	79	+ 60	8.16.0	217	- 167	14.5.0	74	- 52	2.15.$\bar{1}$	63	- 56
0.20.0	292	+ 305	4.17.0	94	+ 91	9 1 0	314	- 335	14.6.0	97	- 89	2.16.$\bar{1}$	79	+ 66
1 1 0	52	- 12	4.18.0	73	- 60	9 2 0	254	+ 264	14.7.0	73	- 51	2.17.$\bar{1}$	92	- 81
1 2 0	173	- 126	4.19.0	268	- 280	9 3 0	123	+ 107	14.8.0	269	+ 222	2.18.$\bar{1}$	85	+ 81
1 3 0	120	+ 83	5 1 0	213	+ 356	9 4 0	261	- 253	14.9.0	153	+ 132	3 1 $\bar{1}$	135	- 158
1 4 0	136	+ 78	5 3 0	114	- 126	9 5 0	92	+ 69	14.10.0	277	+ 234	3 2 $\bar{1}$	121	- 149
1 5 0	88	- 119	5 4 0	26	- 1	9 6 0	77	- 56	15.1.0	36	- 6	3 3 $\bar{1}$	263	+ 288
1 6 0	149	+ 133	5 5 0	31	+ 4	9 7 0	46	- 11	15.2.0	142	+ 120	3 4 $\bar{1}$	263	+ 310
1 7 0	137	+ 122	5 6 0	215	- 212	9 8 0	241	+ 219	15.3.0	187	+ 150	3 5 $\bar{1}$	124	+ 108
1 8 0	196	- 162	5 7 0	33	+ 17	9 9 0	201	+ 168	15.4.0	140	- 95	3 7 $\bar{1}$	308	- 294
1 9 0	88	+ 63	5 8 0	74	+ 71	9.10.0	172	+ 162	15.5.0	22	+ 4	3 9 $\bar{1}$	117	+ 104
1.10.0	328	- 325	5 9 0	265	- 250	9.11.0	183	+ 161	15.6.0	208	- 179	3.10.$\bar{1}$	53	+ 32
1.11.0	112	+ 77	5.10.0	60	+ 44	9.12.0	255	- 239	15.7.0	68	- 66	3.11.$\bar{1}$	274	+ 286
1.12.0	169	+ 173	5.11.0	400	- 419	9.13.0	22	- 17	15.8.0	105	+ 93	3.12.$\bar{1}$	235	+ 208
1.13.0	85	- 66	5.12.0	178	+ 143	9.14.0	200	+ 169	16.0.0	304	+ 244	3.13.$\bar{1}$	51	+ 18
1.14.0	27	- 22	5.13.0	247	+ 231	9.15.0	155	- 129	16.1.0	190	+ 162	3.14.$\bar{1}$	265	- 241
1.15.0	288	+ 264	5.14.0	209	- 193	10.0.0	313	+ 328	16.2.0	126	- 104	3.15.$\bar{1}$	117	+ 55
1.17.0	113	- 117	5.15.0	106	+ 91	10.1.0	267	- 262	16.3.0	278	- 211	3.16.$\bar{1}$	74	+ 71
1.18.0	32	+ 1	5.16.0	218	+ 210	10.2.0	247	+ 234	16.4.0	205	- 170	3.17.$\bar{1}$	182	+ 183
1.19.0	18	- 27	5.17.0	151	+ 119	10.3.0	181	+ 182				3.18.$\bar{1}$	109	- 94
1.20.0	274	+ 293	5.18.0	181	+ 156	10.4.0	36	- 28	0 0 $\bar{1}$	222	+ 245	4 0 $\bar{1}$	200	+ 235
2 0 0	113	- 51	6 0 0	47	- 5	10.5.0	287	- 278	0 1 $\bar{1}$	5	+ 41	4 1 $\bar{1}$	402	+ 684
2 2 0	120	- 125	6 1 0	54	+ 51	10.7.0	96	+ 85	0 2 $\bar{1}$	370	- 374	4 2 $\bar{1}$	322	+ 455
2 3 0	31	- 47	6 2 0	178	+ 210	10.8.0	51	- 33	0 3 $\bar{1}$	85	- 94	4 3 $\bar{1}$	97	+ 98
2 4 0	347	+ 346	6 3 0	54	- 52	10.9.0	65	+ 57	0 4 $\bar{1}$	53	+ 38	4 4 $\bar{1}$	56	- 57
2 5 0	552	+ 768	6 4 0	414	- 512	10.10.0	144	- 123	0 5 $\bar{1}$	147	+ 97	4 5 $\bar{1}$	26	+ 25
2 6 0	319	- 309	6 5 0	47	- 15	10.11.0	265	+ 224	0 6 $\bar{1}$	67	- 50	4 6 $\bar{1}$	155	+ 154
2 7 0	164	- 145	6 6 0	333	+ 345	10.12.0	140	- 91	0 7 $\bar{1}$	242	- 214	4 7 $\bar{1}$	64	- 60
2 8 0	186	+ 144	6 7 0	36	+ 30	10.13.0	229	- 206	0 8 $\bar{1}$	604	+ 656	4 8 $\bar{1}$	349	- 368
2 9 0	96	- 96	6 8 0	86	- 57	10.14.0	36	+ 26	0 9 $\bar{1}$	47	- 6	4 9 $\bar{1}$	317	+ 339
2.10.0	79	+ 69	6 9 0	41	- 39	11.1.0	270	+ 260	0.10.$\bar{1}$	191	+ 132	4.10.$\bar{1}$	31	+ 4
2.11.0	105	- 88	6.10.0	41	+ 15	11.3.0	187	- 167	0.11.$\bar{1}$	33	+ 1	4.11.$\bar{1}$	314	- 310
2.12.0	119	+ 104	6.11.0	223	- 180	11.4.0	222	- 186	0.12.$\bar{1}$	129	+ 96	4.12.$\bar{1}$	91	- 70
2.13.0	67	+ 69	6.12.0	28	- 11	11.5.0	54	- 38	0.13.$\bar{1}$	22	- 24	4.13.$\bar{1}$	130	- 110
2.14.0	311	- 317	6.13.0	205	+ 204	11.6.0	51	- 30	0.14.$\bar{1}$	45	+ 53	4.14.$\bar{1}$	59	+ 42
2.15.0	351	- 340	6.14.0	361	+ 363	11.7.0	245	+ 232	0.16.$\bar{1}$	120	+ 104	4.15.$\bar{1}$	18	+ 12
2.16.0	46	- 18	6.15.0	46	+ 28	11.8.0	115	- 90	0.17.$\bar{1}$	206	+ 205	4.17.$\bar{1}$	18	+ 5
2.17.0	50	+ 12	6.16.0	36	- 28	11.9.0	170	- 133	0.18.$\bar{1}$	273	- 298	4.18.$\bar{1}$	258	+ 251
2.18.0	59	+ 69	6.17.0	59	- 40	11.10.0	83	+ 55	0.19.$\bar{1}$	38	- 3	5 1 $\bar{1}$	115	- 111
2.19.0	78	+ 79	7 1 0	65	- 63	11.11.0	56	- 31	1 1 $\bar{1}$	12	+ 68	5 2 $\bar{1}$	219	+ 259
3 1 0	119	- 143	7 2 0	153	- 167	11.12.0	126	- 95	1 2 $\bar{1}$	150	- 157	5 3 $\bar{1}$	73	- 85
3 2 0	101	+ 26	7 3 0	181	+ 179	11.13.0	123	+ 106	1 3 $\bar{1}$	294	- 288	5 4 $\bar{1}$	69	- 55
3 3 0	112	+ 107	7 4 0	432	+ 498	11.14.0	228	+ 194	1 4 $\bar{1}$	185	+ 154	5 5 $\bar{1}$	33	+ 42
3 4 0	205	- 207	7 5 0	217	+ 208	12.0.0	245	+ 244	1 5 $\bar{1}$	38	- 25	5 6 $\bar{1}$	162	- 165
3 5 0	310	+ 319	7 6 0	367	+ 454	12.1.0	81	- 67	1 6 $\bar{1}$	246	+ 217	5 7 $\bar{1}$	149	+ 136
3 6 0	411	- 499	7 7 0	141	- 124	12.2.0	38	- 37	1 7 $\bar{1}$	532	+ 535	5 8 $\bar{1}$	59	+ 56
3 7 0	64	+ 33	7 8 0	131	- 124	12.3.0	168	+ 140	1 8 $\bar{1}$	92	+ 61	5 9 $\bar{1}$	208	+ 193
3 8 0	190	+ 180	7 9 0	228	+ 203	12.4.0	77	+ 64	1 9 $\bar{1}$	146	- 125	5.10.$\bar{1}$	65	- 22
3.10.0	183	- 166	7.10.0	146	- 126	12.5.0	206	+ 187	1.10.$\bar{1}$	156	- 145	5.11.$\bar{1}$	210	- 209
3.11.0	235	+ 226	7.11.0	73	- 56	12.6.0	270	- 233	1.11.$\bar{1}$	82	+ 72	5.12.$\bar{1}$	165	- 146
3.12.0	214	+ 194	7.12.0	26	+ 36	12.7.0	288	+ 238	1.12.$\bar{1}$	250	+ 236	5.13.$\bar{1}$	160	+ 145
3.13.0	19	- 7	7.13.0	104	+ 88	12.8.0	149	+ 133	1.13.$\bar{1}$	62	+ 36	5.14.$\bar{1}$	50	- 34
3.14.0	64	+ 71	7.14.0	246	- 210	12.9.0	247	- 211	1.14.$\bar{1}$	186	- 161	5.16.$\bar{1}$	187	+ 193
3.15.0	231	- 214	7.15.0	65	+ 38	12.10.0	112	- 83	1.15.$\bar{1}$	54	+ 61	5.17.$\bar{1}$	[illegible]	- 4
3.16.0	274	+ 253	7.16.0	249	- 238	12.11.0	63	- 39	1.16.$\bar{1}$	120	- 124	6 0 $\bar{1}$	79	- 62
3.17.0	32	+ 54	7.17.0	163	+ 159	12.13.0	108	- 78	1.17.$\bar{1}$	224	- 226	6 1 $\bar{1}$	149	- 154
3.18.0	141	- 132	8 0 0	295	- 351	13.1.0	58	- 34	1.18.$\bar{1}$	240	- 224	6 2 $\bar{1}$	122	+ 133
3.19.0	176	+ 173	8 1 0	213	- 235	13.2.0	241	- 209	1.19.$\bar{1}$	153	+ 141	6 3 $\bar{1}$	33	+ 64
4 0 0	273	- 373	8 2 0	205	+ 195	13.3.0	129	+ 120	2 0 $\bar{1}$	72	- 53	6 4 $\bar{1}$	372	- 440
4 1 0	279	+ 426	8 3 0	39	+ 34	13.4.0	136	+ 103	2 1 $\bar{1}$	63	- 82	6 5 $\bar{1}$	335	- 357
4 2 0	33	+ 34	8 4 0	40	- 17	13.6.0	94	+ 86	2 2 $\bar{1}$	127	+ 147	6 6 $\bar{1}$	405	+ 493
4 3 0	173	- 184	8 5 0	106	- 108	13.7.0	109	+ 75	2 3 $\bar{1}$	405	- 551	6 8 $\bar{1}$	83	+ 68
4 4 0	117	+ 71	8 6 0	258	+ 230	13.8.0	322	- 273	2 4 $\bar{1}$	123	+ 113	6 9 $\bar{1}$	58	- 54
4 5 0	149	- 122	8 7 0	115	+ 106	13.9.0	141	- 129	2 5 $\bar{1}$	129	+ 122	6.10.$\bar{1}$	33	+ 18

h k l	$\|F_{obs}\|$	F_{calc}	h k l	$\|F_{obs}\|$	F_{calc}	h k l	$\|F_{obs}\|$	F_{calc}	h k l	$\|F_{obs}\|$	F_{calc}	h k l	$\|F_{obs}\|$	F_{calc}
6.11.$\bar{1}$	103	+ 103	11.12.$\bar{1}$	213	− 187	$\bar{2}$.15.$\bar{1}$	54	+ 42	$\bar{7}$ 7 $\bar{1}$	51	− 62	$\overline{12}$.11.$\bar{1}$	390	− 338
6.12.$\bar{1}$	179	+ 157	11.13.$\bar{1}$	28	+ 28	$\bar{2}$.16.$\bar{1}$	79	+ 56	$\bar{7}$ 8 $\bar{1}$	191	+ 158	$\overline{12}$.12.$\bar{1}$	158	+ 123
6.13.$\bar{1}$	73	− 44	12.0.$\bar{1}$	377	+ 406	$\bar{2}$.17.$\bar{1}$	73	+ 65	$\bar{7}$ 9 $\bar{1}$	50	+ 64	$\overline{13}$.1.$\bar{1}$	68	+ 28
6.14.$\bar{1}$	190	+ 176	12.1.$\bar{1}$	195	− 159	$\bar{2}$.18.$\bar{1}$	140	+ 126	$\bar{7}$.10.$\bar{1}$	73	+ 74	$\overline{13}$.2.$\bar{1}$	123	− 90
6.15.$\bar{1}$	178	− 177	12.2.$\bar{1}$	268	− 247	$\bar{2}$.19.$\bar{1}$	46	− 51	$\bar{7}$.11.$\bar{1}$	33	− 3	$\overline{13}$.3.$\bar{1}$	237	+ 200
6.16.$\bar{1}$	232	− 197	12.3.$\bar{1}$	161	− 150	$\bar{3}$ 1 $\bar{1}$	53	− 61	$\bar{7}$.12.$\bar{1}$	153	− 243	$\overline{13}$.4.$\bar{1}$	53	− 43
7 1 $\bar{1}$	99	+ 104	12.4.$\bar{1}$	26	− 9	$\bar{3}$ 2 $\bar{1}$	267	− 358	$\bar{7}$.13.$\bar{1}$	206	+ 332	$\overline{13}$.5.$\bar{1}$	53	− 44
7 2 $\bar{1}$	224	− 239	12.5.$\bar{1}$	50	− 24	$\bar{3}$ 3 $\bar{1}$	424	+ 615	$\bar{7}$.14.$\bar{1}$	183	− 154	$\overline{13}$.6.$\bar{1}$	170	− 135
7 3 $\bar{1}$	47	+ 39	12.6.$\bar{1}$	26	− 28	$\bar{3}$ 4 $\bar{1}$	300	− 342	$\bar{7}$.15.$\bar{1}$	112	− 104	$\overline{13}$.7.$\bar{1}$	117	− 99
7 4 $\bar{1}$	335	− 333	12.8.$\bar{1}$	308	+ 261	$\bar{3}$ 5 $\bar{1}$	38	+ 39	$\bar{7}$.16.$\bar{1}$	53	+ 64	$\overline{13}$.8.$\bar{1}$	138	− 89
7 5 $\bar{1}$	272	+ 256	12.9.$\bar{1}$	181	− 161	$\bar{3}$ 6 $\bar{1}$	18	− 16	$\bar{8}$ 0 $\bar{1}$	222	− 227	$\overline{13}$.9.$\bar{1}$	205	− 139
7 6 $\bar{1}$	32	+ 1	12.10.$\bar{1}$	245	− 235	$\bar{3}$ 7 $\bar{1}$	324	− 341	$\bar{8}$ 1 $\bar{1}$	59	− 49	$\overline{13}$.10.$\bar{1}$	47	+ 35
7 8 $\bar{1}$	163	− 145	12.11.$\bar{1}$	129	+ 119	$\bar{3}$ 8 $\bar{1}$	260	− 254	$\bar{8}$ 2 $\bar{1}$	308	+ 345	$\overline{13}$.11.$\bar{1}$	182	+ 151
7 9 $\bar{1}$	81	+ 67	12.12.$\bar{1}$	147	+ 105	$\bar{3}$ 9 $\bar{1}$	33	− 6	$\bar{8}$ 3 $\bar{1}$	109	− 109	$\overline{14}$.0.$\bar{1}$	188	+ 160
7.10.$\bar{1}$	18	− 32	13.1.$\bar{1}$	228	− 200	$\bar{3}$.10.$\bar{1}$	79	+ 61	$\bar{8}$ 4 $\bar{1}$	78	+ 74	$\overline{14}$.1.$\bar{1}$	41	+ 9
7.11.$\bar{1}$	181	− 169	13.2.$\bar{1}$	195	− 162	$\bar{3}$.11.$\bar{1}$	190	+ 176	$\bar{8}$ 6 $\bar{1}$	88	− 79	$\overline{14}$.2.$\bar{1}$	77	+ 52
7.12.$\bar{1}$	145	+ 127	13.3.$\bar{1}$	178	+ 158	$\bar{3}$.12.$\bar{1}$	138	+ 111	$\bar{8}$ 7 $\bar{1}$	251	− 225	$\overline{14}$.3.$\bar{1}$	112	− 87
7.13.$\bar{1}$	124	+ 111	13.4.$\bar{1}$	26	− 2	$\bar{3}$.13.$\bar{1}$	238	− 222	$\bar{8}$ 8 $\bar{1}$	423	− 396	$\overline{14}$.4.$\bar{1}$	376	+ 323
7.14.$\bar{1}$	378	+ 370	13.5.$\bar{1}$	64	− 69	$\bar{3}$.14.$\bar{1}$	236	+ 211	$\bar{8}$ 9 $\bar{1}$	50	+ 18	$\overline{14}$.5.$\bar{1}$	91	+ 77
7.15.$\bar{1}$	83	+ 41	13.6.$\bar{1}$	53	+ 39	$\bar{3}$.15.$\bar{1}$	210	+ 178	$\bar{8}$.10.$\bar{1}$	277	+ 251	$\overline{14}$.6.$\bar{1}$	354	− 279
7.16.$\bar{1}$	147	− 169	13.7.$\bar{1}$	26	− 30	$\bar{3}$.17.$\bar{1}$	174	+ 169	$\bar{8}$.11.$\bar{1}$	131	+ 103	$\overline{14}$.7.$\bar{1}$	63	+ 61
8 0 $\bar{1}$	314	− 378	13.8.$\bar{1}$	41	+ 25	$\bar{3}$.18.$\bar{1}$	153	+ 137	$\bar{8}$.12.$\bar{1}$	118	− 96	$\overline{15}$.1.$\bar{1}$	54	− 50
8 1 $\bar{1}$	285	− 310	13.9.$\bar{1}$	154	+ 131	$\bar{4}$ 0 $\bar{1}$	259	+ 298	$\bar{8}$.13.$\bar{1}$	150	+ 134	$\overline{15}$.2.$\bar{1}$	227	− 186
8 2 $\bar{1}$	156	+ 150	13.10.$\bar{1}$	73	− 51	$\bar{4}$ 1 $\bar{1}$	328	− 477	$\bar{8}$.14.$\bar{1}$	50	+ 15	$\overline{15}$.3.$\bar{1}$	135	− 102
8 3 $\bar{1}$	62	− 28	13.11.$\bar{1}$	244	+ 214	$\bar{4}$ 2 $\bar{1}$	46	− 29	$\bar{8}$.15.$\bar{1}$	26	+ 19	$\overline{15}$.4.$\bar{1}$	186	− 140
8 4 $\bar{1}$	118	+ 112	14.0.$\bar{1}$	367	+ 313	$\bar{4}$ 3 $\bar{1}$	137	+ 147	$\bar{9}$ 1 $\bar{1}$	76	− 61	$\overline{15}$.5.$\bar{1}$	47	+ 31
8 5 $\bar{1}$	92	− 74	14.1.$\bar{1}$	67	+ 38	$\bar{4}$ 4 $\bar{1}$	51	+ 12	$\bar{9}$ 2 $\bar{1}$	63	− 69	$\overline{15}$.6.$\bar{1}$	85	+ 64
8 6 $\bar{1}$	104	− 86	14.2.$\bar{1}$	87	+ 60	$\bar{4}$ 5 $\bar{1}$	129	− 97	$\bar{9}$ 3 $\bar{1}$	170	+ 141	$\overline{15}$.7.$\bar{1}$	227	+ 176
8 7 $\bar{1}$	118	+ 98	14.3.$\bar{1}$	59	− 29	$\bar{4}$ 6 $\bar{1}$	167	+ 182	$\bar{9}$ 4 $\bar{1}$	28	+ 37			
8 8 $\bar{1}$	154	− 145	14.4.$\bar{1}$	305	+ 270	$\bar{4}$ 7 $\bar{1}$	345	+ 370	$\bar{9}$ 5 $\bar{1}$	83	+ 62	0 0 $\bar{2}$	602	+ 700
8 9 $\bar{1}$	247	− 237	14.5.$\bar{1}$	191	+ 165	$\bar{4}$ 8 $\bar{1}$	76	+ 47	$\bar{9}$ 6 $\bar{1}$	88	+ 73	0 1 $\bar{2}$	212	+ 442
8.10.$\bar{1}$	327	+ 331	14.6.$\bar{1}$	251	− 211	$\bar{4}$ 9 $\bar{1}$	270	− 289	$\bar{9}$ 7 $\bar{1}$	246	− 215	0 2 $\bar{2}$	58	− 114
8.11.$\bar{1}$	267	+ 245	14.7.$\bar{1}$	110	− 92	$\bar{4}$.10.$\bar{1}$	51	− 44	$\bar{9}$ 8 $\bar{1}$	186	+ 135	0 3 $\bar{2}$	109	− 115
8.12.$\bar{1}$	69	+ 51	14.8.$\bar{1}$	115	− 98	$\bar{4}$.11.$\bar{1}$	227	+ 214	$\bar{9}$ 9 $\bar{1}$	109	+ 75	0 4 $\bar{2}$	13	+ 8
8.13.$\bar{1}$	30	− 32	14.9.$\bar{1}$	126	+ 97	$\bar{4}$.12.$\bar{1}$	47	+ 38	$\bar{9}$.10.$\bar{1}$	142	− 136	0 5 $\bar{2}$	58	− 37
8.14.$\bar{1}$	50	+ 12	15.1.$\bar{1}$	60	+ 37	$\bar{4}$.13.$\bar{1}$	74	+ 73	$\bar{9}$.11.$\bar{1}$	109	− 77	0 6 $\bar{2}$	40	− 38
8.15.$\bar{1}$	31	+ 24	15.2.$\bar{1}$	141	+ 182	$\bar{4}$.16.$\bar{1}$	96	− 79	$\bar{9}$.12.$\bar{1}$	226	+ 192	0 7 $\bar{2}$	26	+ 23
9 1 $\bar{1}$	144	+ 113	15.3.$\bar{1}$	65	+ 25	$\bar{4}$.17.$\bar{1}$	270	− 259	$\bar{9}$.13.$\bar{1}$	87	+ 52	0 8 $\bar{2}$	273	+ 263
9 2 $\bar{1}$	42	+ 85	15.4.$\bar{1}$	65	− 63	$\bar{4}$.18.$\bar{1}$	64	+ 40	$\bar{9}$.14.$\bar{1}$	42	+ 25	0 9 $\bar{2}$	350	+ 339
9 3 $\bar{1}$	185	+ 168	15.5.$\bar{1}$	60	+ 37	$\bar{5}$ 1 $\bar{1}$	94	+ 103	$\overline{10}$.0.$\bar{1}$	26	+ 29	0.10.$\bar{2}$	236	− 217
9 4 $\bar{1}$	28	− 22	15.6.$\bar{1}$	229	− 204	$\bar{5}$ 2 $\bar{1}$	231	− 277	$\overline{10}$.2.$\bar{1}$	146	− 123	0.11.$\bar{2}$	159	− 172
9 5 $\bar{1}$	58	+ 54	15.7.$\bar{1}$	53	− 29	$\bar{5}$ 3 $\bar{1}$	288	− 348	$\overline{10}$.3.$\bar{1}$	370	− 358	0.12.$\bar{2}$	46	+ 70
9 6 $\bar{1}$	62	+ 73	$\bar{1}$ 1 $\bar{1}$	146	+ 204	$\bar{5}$ 4 $\bar{1}$	67	+ 9	$\overline{10}$.4.$\bar{1}$	285	− 242	0.13.$\bar{2}$	92	+ 47
9 7 $\bar{1}$	264	− 229	$\bar{1}$ 2 $\bar{1}$	361	+ 443	$\bar{5}$ 5 $\bar{1}$	109	+ 104	$\overline{10}$.5.$\bar{1}$	327	+ 283	0.14.$\bar{2}$	41	+ 97
9 8 $\bar{1}$	62	− 49	$\bar{1}$ 3 $\bar{1}$	126	+ 86	$\bar{5}$ 6 $\bar{1}$	68	+ 47	$\overline{10}$.6.$\bar{1}$	350	+ 281	1 1 $\bar{2}$	214	+ 345
9 9 $\bar{1}$	292	− 270	$\bar{1}$ 5 $\bar{1}$	79	− 79	$\bar{5}$ 7 $\bar{1}$	358	+ 380	$\overline{10}$.7.$\bar{1}$	349	− 294	1 2 $\bar{2}$	355	− 356
9.10.$\bar{1}$	203	+ 170	$\bar{1}$ 6 $\bar{1}$	193	− 157	$\bar{5}$ 8 $\bar{1}$	228	− 223	$\overline{10}$.8.$\bar{1}$	303	+ 263	1 3 $\bar{2}$	141	+ 117
9.11.$\bar{1}$	73	− 43	$\bar{1}$ 7 $\bar{1}$	147	+ 118	$\bar{5}$ 9 $\bar{1}$	146	+ 124	$\overline{10}$.9.$\bar{1}$	88	− 58	1 4 $\bar{2}$	72	+ 46
9.12.$\bar{1}$	274	− 258	$\bar{1}$ 8 $\bar{1}$	360	+ 347	$\bar{5}$.10.$\bar{1}$	104	+ 87	$\overline{10}$.10.$\bar{1}$	167	+ 114	1 5 $\bar{2}$	147	− 128
9.13.$\bar{1}$	79	+ 50	$\bar{1}$ 9 $\bar{1}$	308	− 283	$\bar{5}$.11.$\bar{1}$	178	− 180	$\overline{10}$.11.$\bar{1}$	150	+ 101	1 8 $\bar{2}$	223	− 194
9.14.$\bar{1}$	42	+ 26	$\bar{1}$.10.$\bar{1}$	86	− 62	$\bar{5}$.13.$\bar{1}$	212	+ 193	$\overline{10}$.12.$\bar{1}$	177	+ 136	1 9 $\bar{2}$	155	− 123
10.0.$\bar{1}$	100	+ 83	$\bar{1}$.11.$\bar{1}$	33	+ 24	$\bar{5}$.14.$\bar{1}$	108	+ 104	$\overline{10}$.13.$\bar{1}$	288	+ 243	1.10.$\bar{2}$	123	− 113
10.1.$\bar{1}$	62	+ 50	$\bar{1}$.12.$\bar{1}$	374	− 372	$\bar{5}$.15.$\bar{1}$	72	− 35	$\overline{11}$.1.$\bar{1}$	117	+ 121	1.11.$\bar{2}$	244	− 223
10.2.$\bar{1}$	118	− 99	$\bar{1}$.13.$\bar{1}$	209	− 165	$\bar{5}$.16.$\bar{1}$	83	− 67	$\overline{11}$.2.$\bar{1}$	31	+ 39	1.12.$\bar{2}$	297	+ 272
10.3.$\bar{1}$	286	− 278	$\bar{1}$.14.$\bar{1}$	18	− 6	$\bar{5}$.17.$\bar{1}$	168	− 168	$\overline{11}$.3.$\bar{1}$	64	− 57	1.14.$\bar{2}$	122	− 120
10.4.$\bar{1}$	112	+ 98	$\bar{1}$.15.$\bar{1}$	223	+ 202	$\bar{6}$ 0 $\bar{1}$	38	− 42	$\overline{11}$.4.$\bar{1}$	78	+ 58	2 1 $\bar{2}$	94	+ 102
10.5.$\bar{1}$	432	− 449	$\bar{1}$.16.$\bar{1}$	145	+ 149	$\bar{6}$ 1 $\bar{1}$	122	+ 126	$\overline{11}$.5.$\bar{1}$	47	+ 27	2 2 $\bar{2}$	64	− 65
10.6.$\bar{1}$	142	− 119	$\bar{1}$.17.$\bar{1}$	114	− 106	$\bar{6}$ 2 $\bar{1}$	301	+ 353	$\overline{11}$.6.$\bar{1}$	73	− 52	2 3 $\bar{2}$	141	− 152
10.7.$\bar{1}$	199	+ 163	$\bar{1}$.18.$\bar{1}$	47	+ 37	$\bar{6}$ 3 $\bar{1}$	345	+ 402	$\overline{11}$.7.$\bar{1}$	182	+ 149	2 4 $\bar{2}$	101	− 108
10.8.$\bar{1}$	206	+ 191	$\bar{1}$.19.$\bar{1}$	188	+ 237	$\bar{6}$ 4 $\bar{1}$	117	− 122	$\overline{11}$.8.$\bar{1}$	46	+ 48	2 5 $\bar{2}$	473	+ 544
10.9.$\bar{1}$	33	+ 42	$\bar{2}$ 0 $\bar{1}$	150	+ 146	$\bar{6}$ 5 $\bar{1}$	265	− 278	$\overline{11}$.9.$\bar{1}$	131	+ 92	2 7 $\bar{2}$	219	− 187
10.10.$\bar{1}$	144	+ 97	$\bar{2}$ 1 $\bar{1}$	96	− 123	$\bar{6}$ 6 $\bar{1}$	113	+ 123	$\overline{11}$.10.$\bar{1}$	79	− 67	2 9 $\bar{2}$	49	− 64
10.11.$\bar{1}$	176	− 142	$\bar{2}$ 2 $\bar{1}$	144	− 184	$\bar{6}$ 7 $\bar{1}$	242	+ 226	$\overline{11}$.11.$\bar{1}$	186	− 156	2.10.$\bar{2}$	73	+ 77
10.12.$\bar{1}$	106	+ 76	$\bar{2}$ 3 $\bar{1}$	258	+ 307	$\bar{6}$ 8 $\bar{1}$	45	− 30	$\overline{11}$.12.$\bar{1}$	65	+ 34	2.11.$\bar{2}$	208	− 174
10.13.$\bar{1}$	210	− 177	$\bar{2}$ 4 $\bar{1}$	173	+ 199	$\bar{6}$.11.$\bar{1}$	113	− 96	$\overline{11}$.13.$\bar{1}$	69	− 36	2.12.$\bar{2}$	47	+ 143
11.1.$\bar{1}$	42	+ 32	$\bar{2}$ 5 $\bar{1}$	172	− 162	$\bar{6}$.12.$\bar{1}$	337	− 301	$\overline{12}$.0.$\bar{1}$	158	+ 144	2.13.$\bar{2}$	190	+ 196
11.2.$\bar{1}$	104	+ 64	$\bar{2}$ 6 $\bar{1}$	296	− 289	$\bar{6}$.13.$\bar{1}$	258	− 240	$\overline{12}$.1.$\bar{1}$	437	+ 425	3 1 $\bar{2}$	71	− 76
11.3.$\bar{1}$	181	− 163	$\bar{2}$ 7 $\bar{1}$	173	+ 147	$\bar{6}$.14.$\bar{1}$	100	+ 104	$\overline{12}$.2.$\bar{1}$	213	− 191	3 2 $\bar{2}$	137	+ 154
11.4.$\bar{1}$	196	+ 155	$\bar{2}$ 8 $\bar{1}$	42	+ 25	$\bar{6}$.15.$\bar{1}$	100	+ 113	$\overline{12}$.3.$\bar{1}$	123	+ 93	3 3 $\bar{2}$	249	+ 293
11.5.$\bar{1}$	41	+ 27	$\bar{2}$ 9 $\bar{1}$	31	− 18	$\bar{7}$ 1 $\bar{1}$	53	+ 48	$\overline{12}$.4.$\bar{1}$	58	− 23	3 4 $\bar{2}$	91	+ 97
11.6.$\bar{1}$	244	+ 204	$\bar{2}$.10.$\bar{1}$	51	− 33	$\bar{7}$ 2 $\bar{1}$	322	+ 363	$\overline{12}$.5.$\bar{1}$	38	+ 25	3 5 $\bar{2}$	236	+ 222
11.7.$\bar{1}$	344	+ 305	$\bar{2}$.11.$\bar{1}$	36	+ 22	$\bar{7}$ 3 $\bar{1}$	67	− 67	$\overline{12}$.6.$\bar{1}$	95	− 79	3 7 $\bar{2}$	296	− 296
11.8.$\bar{1}$	32	− 22	$\bar{2}$.12.$\bar{1}$	388	+ 386	$\bar{7}$ 4 $\bar{1}$	113	+ 110	$\overline{12}$.8.$\bar{1}$	205	+ 161	3 8 $\bar{2}$	177	+ 180
11.9.$\bar{1}$	137	+ 95	$\bar{2}$.13.$\bar{1}$	274	− 264	$\bar{7}$ 5 $\bar{1}$	264	+ 257	$\overline{12}$.9.$\bar{1}$	348	+ 291	3 9 $\bar{2}$	156	+ 163
11.10.$\bar{1}$	82	+ 82	$\bar{2}$.14.$\bar{1}$	164	− 163	$\bar{7}$ 6 $\bar{1}$	71	+ 41	$\overline{12}$.10.$\bar{1}$	36	+ 5	3.10.$\bar{2}$	246	− 230

h k l	$\lvert F_{obs} \rvert$	F_{calc}
$3.11.\bar{2}$	33	+ 19
$3.12.\bar{2}$	31	− 3
$3.13.\bar{2}$	96	− 91
4 0 $\bar{2}$	320	− 420
4 1 $\bar{2}$	90	+ 107
4 2 $\bar{2}$	74	+ 92
4 3 $\bar{2}$	138	− 147
4 4 $\bar{2}$	38	− 28
4 5 $\bar{2}$	95	− 113
4 6 $\bar{2}$	218	+ 214
4 7 $\bar{2}$	327	− 352
4 9 $\bar{2}$	85	+ 77
$4.10.\bar{2}$	376	+ 420
$4.11.\bar{2}$	133	+ 123
$4.12.\bar{2}$	31	+ 29
$4.13.\bar{2}$	22	− 6
5 2 $\bar{2}$	177	+ 226
5 3 $\bar{2}$	172	− 208
5 4 $\bar{2}$	113	− 120
5 5 $\bar{2}$	104	+ 85
5 6 $\bar{2}$	182	− 164
5 7 $\bar{2}$	118	+ 110
5 8 $\bar{2}$	249	+ 238
5 9 $\bar{2}$	62	+ 52
$5.10.\bar{2}$	133	+ 108
$5.11.\bar{2}$	199	− 194
$5.12.\bar{2}$	88	− 90
6 0 $\bar{2}$	108	+ 97
6 1 $\bar{2}$	137	− 147
6 2 $\bar{2}$	250	+ 298
6 4 $\bar{2}$	236	− 250
6 5 $\bar{2}$	285	− 291
6 6 $\bar{2}$	97	+ 78
6 8 $\bar{2}$	155	− 127
6 9 $\bar{2}$	76	− 57
$6.10.\bar{2}$	41	− 56
$6.11.\bar{2}$	99	+ 85
7 1 $\bar{2}$	81	+ 69
7 2 $\bar{2}$	195	− 229
7 3 $\bar{2}$	146	− 163
7 4 $\bar{2}$	210	+ 217
7 5 $\bar{2}$	133	+ 141
7 6 $\bar{2}$	315	+ 307
7 7 $\bar{2}$	87	+ 86
7 8 $\bar{2}$	223	− 237
7 9 $\bar{2}$	33	+ 40
$7.11.\bar{2}$	31	− 17
8 0 $\bar{2}$	73	− 74
8 1 $\bar{2}$	154	− 154
8 2 $\bar{2}$	176	+ 163
8 3 $\bar{2}$	301	+ 309
8 4 $\bar{2}$	149	+ 149
8 5 $\bar{2}$	53	+ 20
8 7 $\bar{2}$	347	+ 353
8 8 $\bar{2}$	162	− 141
8 9 $\bar{2}$	274	− 265
$8.10.\bar{2}$	63	+ 52
9 1 $\bar{2}$	299	− 340
9 3 $\bar{2}$	200	+ 228
9 4 $\bar{2}$	92	− 93
9 5 $\bar{2}$	50	+ 41
9 7 $\bar{2}$	41	− 64
9 8 $\bar{2}$	41	− 20
9 9 $\bar{2}$	158	+ 120
$10.0.\bar{2}$	217	+ 217
$10.1.\bar{2}$	73	− 71
$10.2.\bar{2}$	185	− 178
$10.3.\bar{2}$	236	+ 238
$10.4.\bar{2}$	69	+ 52
$10.5.\bar{2}$	213	− 195
$10.6.\bar{2}$	96	+ 83
$10.7.\bar{2}$	181	+ 156
$10.8.\bar{2}$	205	+ 157
$11.1.\bar{2}$	241	+ 228
$11.3.\bar{2}$	101	+ 79

h k l	$\lvert F_{obs} \rvert$	F_{calc}
$11.4.\bar{2}$	295	− 267
$11.5.\bar{2}$	65	− 52
$11.6.\bar{2}$	168	− 141
$12.0.\bar{2}$	279	+ 235
$12.1.\bar{2}$	118	− 97
$12.2.\bar{2}$	106	− 99
$12.3.\bar{2}$	108	− 96
$\bar{1}$ 1 $\bar{2}$	91	− 119
$\bar{1}$ 3 $\bar{2}$	119	− 86
$\bar{1}$ 4 $\bar{2}$	218	− 207
$\bar{1}$ 6 $\bar{2}$	311	− 290
$\bar{1}$ 7 $\bar{2}$	258	+ 212
$\bar{1}$ 8 $\bar{2}$	104	+ 102
$\bar{1}.10.\bar{2}$	214	+ 195
$\bar{1}.11.\bar{2}$	206	+ 190
$\bar{1}.12.\bar{2}$	47	− 44
$\bar{1}.13.\bar{2}$	101	− 81
$\bar{2}$ 0 $\bar{2}$	88	− 116
$\bar{2}$ 2 $\bar{2}$	60	− 64
$\bar{2}$ 3 $\bar{2}$	118	+ 125
$\bar{2}$ 4 $\bar{2}$	415	+ 505
$\bar{2}$ 5 $\bar{2}$	88	+ 39
$\bar{2}$ 6 $\bar{2}$	387	− 402
$\bar{2}$ 7 $\bar{2}$	63	+ 59
$\bar{2}$ 8 $\bar{2}$	144	+ 113
$\bar{2}$ 9 $\bar{2}$	83	+ 70
$\bar{2}.10.\bar{2}$	85	+ 53
$\bar{2}.11.\bar{2}$	41	− 31
$\bar{2}.12.\bar{2}$	31	+ 28
$\bar{2}.13.\bar{2}$	142	− 140
$\bar{3}$ 1 $\bar{2}$	150	− 182
$\bar{3}$ 2 $\bar{2}$	73	+ 74
$\bar{3}$ 3 $\bar{2}$	49	+ 44
$\bar{3}$ 4 $\bar{2}$	67	+ 69
$\bar{3}$ 5 $\bar{2}$	86	+ 106
$\bar{3}$ 6 $\bar{2}$	349	+ 386
$\bar{3}$ 7 $\bar{2}$	173	+ 174
$\bar{3}.10.\bar{2}$	105	− 91
$\bar{3}.11.\bar{2}$	347	+ 359
$\bar{3}.12.\bar{2}$	228	− 193
$\bar{3}.13.\bar{2}$	59	+ 54
$\bar{4}$ 0 $\bar{2}$	273	+ 345
$\bar{4}$ 1 $\bar{2}$	320	− 420
$\bar{4}$ 2 $\bar{2}$	50	+ 40
$\bar{4}$ 4 $\bar{2}$	71	+ 78
$\bar{4}$ 5 $\bar{2}$	100	+ 100
$\bar{4}$ 6 $\bar{2}$	97	− 87
$\bar{4}$ 7 $\bar{2}$	68	+ 59
$\bar{4}$ 9 $\bar{2}$	374	− 389
$\bar{4}.10.\bar{2}$	137	− 125
$\bar{4}.11.\bar{2}$	238	+ 227
$\bar{5}$ 1 $\bar{2}$	59	+ 106
$\bar{5}$ 4 $\bar{2}$	33	− 23
$\bar{5}$ 5 $\bar{2}$	99	− 94
$\bar{5}$ 6 $\bar{2}$	163	+ 148
$\bar{5}$ 7 $\bar{2}$	42	+ 45
$\bar{5}$ 8 $\bar{2}$	41	+ 35
$\bar{5}$ 9 $\bar{2}$	81	− 82
$\bar{5}.10.\bar{2}$	133	+ 122
$\bar{5}.11.\bar{2}$	197	− 199
$\bar{5}.12.\bar{2}$	185	− 166
$\bar{6}$ 1 $\bar{2}$	79	− 75
$\bar{6}$ 3 $\bar{2}$	83	+ 78
$\bar{6}$ 4 $\bar{2}$	314	− 325
$\bar{6}$ 5 $\bar{2}$	483	− 544
$\bar{6}$ 6 $\bar{2}$	364	+ 361
$\bar{6}$ 8 $\bar{2}$	95	+ 69
$\bar{6}.11.\bar{2}$	183	+ 164
$\bar{7}$ 1 $\bar{2}$	88	− 83
$\bar{7}$ 2 $\bar{2}$	90	+ 105
$\bar{7}$ 3 $\bar{2}$	240	+ 256
$\bar{7}$ 4 $\bar{2}$	131	− 111
$\bar{7}$ 5 $\bar{2}$	196	+ 183
$\bar{7}$ 6 $\bar{2}$	88	− 81
$\bar{7}$ 7 $\bar{2}$	126	− 117

h k l	$\lvert F_{obs} \rvert$	F_{calc}
$\bar{7}$ 8 $\bar{2}$	38	− 32
$\bar{7}$ 9 $\bar{2}$	156	+ 136
$\bar{7}.10.\bar{2}$	200	+ 177
$\bar{8}$ 0 $\bar{2}$	465	− 557
$\bar{8}$ 2 $\bar{2}$	91	+ 128
$\bar{8}$ 3 $\bar{2}$	187	+ 174
$\bar{8}$ 6 $\bar{2}$	146	+ 128
$\bar{8}$ 7 $\bar{2}$	113	+ 75
$\bar{8}$ 8 $\bar{2}$	195	− 144
$\bar{8}$ 9 $\bar{2}$	67	− 52
$\bar{8}.10.\bar{2}$	460	+ 452
$\bar{9}$ 1 $\bar{2}$	132	+ 130
$\bar{9}$ 2 $\bar{2}$	250	− 244
$\bar{9}$ 3 $\bar{2}$	26	− 29
$\bar{9}$ 4 $\bar{2}$	176	+ 152
$\bar{9}$ 5 $\bar{2}$	103	+ 68
$\bar{9}$ 6 $\bar{2}$	53	+ 36
$\bar{9}$ 7 $\bar{2}$	67	− 52
$\bar{9}$ 8 $\bar{2}$	213	− 195
$\overline{10}.0.\bar{2}$	101	+ 119
$\overline{10}.1.\bar{2}$	105	+ 100
$\overline{10}.2.\bar{2}$	341	+ 328
$\overline{10}.3.\bar{2}$	41	− 38
$\overline{10}.4.\bar{2}$	169	− 153
$\overline{10}.5.\bar{2}$	316	+ 283
$\overline{10}.6.\bar{2}$	28	+ 28
$\overline{10}.7.\bar{2}$	59	− 30
$\overline{10}.8.\bar{2}$	79	− 44
$\overline{11}.1.\bar{2}$	140	+ 132
$\overline{11}.2.\bar{2}$	46	+ 21
$\overline{11}.3.\bar{2}$	191	− 156
$\overline{11}.4.\bar{2}$	201	− 173
$\overline{11}.6.\bar{2}$	249	− 219
$\overline{12}.0.\bar{2}$	212	+ 175
$\overline{12}.2.\bar{2}$	22	− 12
$\overline{12}.3.\bar{2}$	96	− 88
0 0 $\bar{3}$	181	+ 432
0 1 $\bar{3}$	100	+ 177
0 3 $\bar{3}$	76	− 79
0 4 $\bar{3}$	85	− 56
0 5 $\bar{3}$	142	+ 127
0 6 $\bar{3}$	38	+ 50
0 7 $\bar{3}$	245	− 220
0 8 $\bar{3}$	169	+ 136
0 9 $\bar{3}$	96	+ 82
1 1 $\bar{3}$	87	− 78
1 2 $\bar{3}$	64	+ 41
1 3 $\bar{3}$	224	− 210
1 4 $\bar{3}$	22	+ 38
1 5 $\bar{3}$	99	− 41
1 6 $\bar{3}$	36	− 16
1 7 $\bar{3}$	332	+ 352
1 8 $\bar{3}$	201	+ 192
1 9 $\bar{3}$	153	+ 190
$1.10.\bar{3}$	245	− 249
2 0 $\bar{3}$	119	− 143
2 1 $\bar{3}$	46	− 59
2 2 $\bar{3}$	117	+ 140
2 3 $\bar{3}$	186	− 173
2 4 $\bar{3}$	236	− 93
2 6 $\bar{3}$	73	+ 38
2 7 $\bar{3}$	162	− 143
2 8 $\bar{3}$	42	− 39
$2.10.\bar{3}$	132	+ 114
3 1 $\bar{3}$	64	− 38
3 2 $\bar{3}$	190	− 247
3 3 $\bar{3}$	36	+ 9
3 4 $\bar{3}$	110	− 76
3 5 $\bar{3}$	82	+ 142
3 6 $\bar{3}$	115	− 103
3 7 $\bar{3}$	106	− 110
3 8 $\bar{3}$	73	− 73
3 9 $\bar{3}$	53	+ 56
4 0 $\bar{3}$	213	− 273

h k l	$\lvert F_{obs} \rvert$	F_{calc}
4 1 $\bar{3}$	205	+ 280
4 2 $\bar{3}$	290	+ 379
4 3 $\bar{3}$	138	+ 156
4 4 $\bar{3}$	62	+ 5
4 7 $\bar{3}$	88	+ 95
4 8 $\bar{3}$	245	− 241
4 9 $\bar{3}$	165	+ 164
5 1 $\bar{3}$	162	+ 176
5 2 $\bar{3}$	109	+ 122
5 3 $\bar{3}$	54	+ 60
5 6 $\bar{3}$	96	− 99
5 7 $\bar{3}$	79	− 72
5 9 $\bar{3}$	123	− 117
6 0 $\bar{3}$	46	+ 6
6 1 $\bar{3}$	41	− 37
6 3 $\bar{3}$	227	+ 257
6 4 $\bar{3}$	224	− 341
6 5 $\bar{3}$	58	− 65
6 6 $\bar{3}$	310	+ 347
6 7 $\bar{3}$	117	+ 93
6 8 $\bar{3}$	60	+ 80
7 2 $\bar{3}$	69	− 50
7 3 $\bar{3}$	99	+ 110
7 4 $\bar{3}$	36	+ 1
7 5 $\bar{3}$	108	+ 95
7 6 $\bar{3}$	227	+ 234
7 7 $\bar{3}$	256	+ 60
8 0 $\bar{3}$	87	− 63
8 1 $\bar{3}$	288	− 325
8 2 $\bar{3}$	46	− 32
8 3 $\bar{3}$	115	− 116
8 4 $\bar{3}$	92	+ 89
8 5 $\bar{3}$	164	− 128
8 6 $\bar{3}$	50	+ 51
8 7 $\bar{3}$	26	− 46
9 1 $\bar{3}$	63	− 102
9 3 $\bar{3}$	126	+ 121
$\underline{9}$ 4 $\bar{3}$	122	− 96
$\bar{1}$ 2 $\bar{3}$	145	+ 171
$\bar{1}$ 3 $\bar{3}$	141	+ 148
$\bar{1}$ 4 $\bar{3}$	64	+ 75
$\bar{1}$ 5 $\bar{3}$	79	− 62
$\bar{1}$ 6 $\bar{3}$	88	− 71
$\bar{1}$ 7 $\bar{3}$	146	− 136
$\bar{1}$ 8 $\bar{3}$	262	+ 289
$\bar{1}$ 9 $\bar{3}$	64	− 46
$\bar{1}.10.\bar{3}$	38	− 34
$\bar{2}$ 0 $\bar{3}$	96	+ 96
$\bar{2}$ 1 $\bar{3}$	13	+ 14
$\bar{2}$ 2 $\bar{3}$	122	− 151
$\bar{2}$ 3 $\bar{3}$	112	− 140
$\bar{2}$ 4 $\bar{3}$	222	+ 266
$\bar{2}$ 5 $\bar{3}$	261	− 297
$\bar{2}$ 6 $\bar{3}$	228	− 236
$\bar{2}$ 7 $\bar{3}$	44	− 80
$\bar{2}$ 8 $\bar{3}$	36	+ 17
$\bar{2}$ 9 $\bar{3}$	76	+ 63
$\bar{2}.10.\bar{3}$	28	− 39
$\bar{3}$ 2 $\bar{3}$	247	− 347
$\bar{3}$ 3 $\bar{3}$	164	+ 265
$\bar{3}$ 5 $\bar{3}$	45	+ 61
$\bar{3}$ 6 $\bar{3}$	136	+ 157
$\bar{3}$ 8 $\bar{3}$	169	− 178
$\bar{3}$ 9 $\bar{3}$	79	− 88
$\bar{4}$ 0 $\bar{3}$	67	+ 56
$\bar{4}$ 1 $\bar{3}$	144	− 172
$\bar{4}$ 2 $\bar{3}$	210	− 277
$\bar{4}$ 3 $\bar{3}$	74	+ 83
$\bar{4}$ 4 $\bar{3}$	145	+ 111
$\bar{4}$ 7 $\bar{3}$	181	+ 174
$\bar{4}$ 8 $\bar{3}$	296	+ 333
$\bar{4}$ 9 $\bar{3}$	212	− 206
$\bar{5}$ 1 $\bar{3}$	146	+ 166
$\bar{5}$ 2 $\bar{3}$	41	+ 58
$\bar{5}$ 3 $\bar{3}$	199	− 207

h k l	$\lvert F_{obs} \rvert$	F_{calc}
$\bar{5}$ 4 $\bar{3}$	59	− 46
$\bar{5}$ 5 $\bar{3}$	59	+ 53
$\bar{5}$ 7 $\bar{3}$	214	+ 210
$\bar{5}$ 9 $\bar{3}$	168	− 170
$\bar{6}$ 0 $\bar{3}$	50	+ 25
$\bar{6}$ 1 $\bar{3}$	47	− 28
$\bar{6}$ 2 $\bar{3}$	120	+ 126
$\bar{6}$ 3 $\bar{3}$	345	+ 417
$\bar{6}$ 4 $\bar{3}$	50	+ 56
$\bar{6}$ 5 $\bar{3}$	42	− 37
$\bar{6}$ 6 $\bar{3}$	74	− 65
$\bar{6}$ 7 $\bar{3}$	163	+ 149
$\bar{7}$ 2 $\bar{3}$	155	+ 156
$\bar{7}$ 3 $\bar{3}$	132	+ 125
$\bar{7}$ 4 $\bar{3}$	233	− 226
$\bar{7}$ 5 $\bar{3}$	118	+ 105
$\bar{7}$ 6 $\bar{3}$	85	− 90
$\bar{7}$ 7 $\bar{3}$	169	− 155
$\bar{8}$ 0 $\bar{3}$	73	− 37
$\bar{8}$ 1 $\bar{3}$	118	− 111
$\bar{8}$ 2 $\bar{3}$	158	+ 171
$\bar{8}$ 6 $\bar{3}$	96	+ 65
$\bar{9}$ 1 $\bar{3}$	217	+ 210
$\bar{9}$ 2 $\bar{3}$	192	− 171
0 1 $\bar{4}$	179	+ 285
0 2 $\bar{4}$	26	− 38
0 3 $\bar{4}$	128	− 163
0 4 $\bar{4}$	45	− 24
0 6 $\bar{4}$	42	+ 48
0 7 $\bar{4}$	109	− 118
1 1 $\bar{4}$	135	+ 290
1 2 $\bar{4}$	138	− 161
1 3 $\bar{4}$	91	− 90
1 4 $\bar{4}$	54	+ 55
2 2 $\bar{4}$	104	+ 140
2 3 $\bar{4}$	165	− 200
2 4 $\bar{4}$	112	− 152
2 5 $\bar{4}$	69	+ 64
2 6 $\bar{4}$	22	+ 24
3 1 $\bar{4}$	41	− 57
3 3 $\bar{4}$	101	+ 127
3 4 $\bar{4}$	106	+ 171
3 5 $\bar{4}$	47	+ 70
4 0 $\bar{4}$	46	− 67
4 1 $\bar{4}$	31	+ 50
4 2 $\bar{4}$	124	+ 169
4 3 $\bar{4}$	77	+ 80
5 1 $\bar{4}$	131	− 189
5 2 $\bar{4}$	106	+ 158
5 3 $\bar{4}$	47	− 48
$\bar{1}$ 2 $\bar{4}$	71	+ 97
$\bar{1}$ 3 $\bar{4}$	28	+ 39
$\bar{1}$ 4 $\bar{4}$	64	− 96
$\bar{1}$ 5 $\bar{4}$	41	+ 55
$\bar{1}$ 6 $\bar{4}$	88	− 125
$\bar{2}$ 1 $\bar{4}$	31	+ 30
$\bar{2}$ 2 $\bar{4}$	54	− 96
$\bar{2}$ 3 $\bar{4}$	38	+ 58
$\bar{2}$ 4 $\bar{4}$	146	+ 211
$\bar{2}$ 5 $\bar{4}$	196	+ 358
$\bar{2}$ 6 $\bar{4}$	99	− 132
$\bar{3}$ 2 $\bar{4}$	53	− 92
$\bar{3}$ 3 $\bar{4}$	96	+ 174
$\bar{3}$ 4 $\bar{4}$	28	− 60
$\bar{3}$ 6 $\bar{4}$	33	− 42
$\bar{4}$ 0 $\bar{4}$	227	+ 385
$\bar{4}$ 1 $\bar{4}$	68	− 94
$\bar{4}$ 2 $\bar{4}$	45	− 47
$\bar{5}$ 1 $\bar{4}$	46	− 87
$\bar{5}$ 2 $\bar{4}$	63	− 82
$\bar{5}$ 3 $\bar{4}$	87	− 112

This Sb_3S_7 group, then, with its centrosymmetrically equivalent group related by inversion centers at ($\frac{1}{2}$, 0, 0) or (0, $\frac{1}{2}$, 0), can be regarded as forming a large Sb_6S_{14} group. The interatomic distance between these two Sb_3S_7 groups is not less than 3.3 Å, so that only a weaker type of chemical bonding occurs between them. If considered in this large group, each Sb atom has altogether 7 S atoms; that is, three at about 2.5 Å, two at about 3.0 Å, and two at greater than 3.3 Å distances. The two such Sb_6S_{14} groups in the unit cell located around inversion centers provide interstices of three kinds; these are occupied by Fe and by two kinds of Pb atoms.

Six S atoms around the inversion centers at (0, 0, 0) and ($\frac{1}{2}$, $\frac{1}{2}$, 0) surround the Fe atom at the center in a distorted octahedral coordination. The Fe—S distances are 2.36 Å (2), 2.57 Å (2), and 2.66 Å (2), and are similar to those observed in berthierite[5], $FeSb_2S_4$ (2 S at 2.49 Å, 1 S at 2.45 Å, 1 S at 2.46 Å, and 2 S at 2.64 Å). As in the latter mineral, the Fe—S bonds are regarded as largely ionic in their nature.

In two other kinds of interstices provided by the Sb_6S_{14} groups, two kinds of Pb atoms are located. The coordinations of both Pb_I and Pb_{II} can be regarded, to a first approximation, as distorted octahedra if six S atoms at distances less than 3.1 Å are counted. In Fig. 19 these distances are drawn in full lines. As indicated by broken lines in Fig. 19, Pb_I has two additional S atoms at about 3.3 Å, and Pb_{II} has an additional one at 3.3 Å. Counting these additional ones, the coordination numbers are 8 for Pb_I, and 7 for Pb_{II}. Both of these two types of Pb atoms were described in the structures of bournonite[15], $CuPbSbS_3$, and seligmannite[15], $CuPbAsS_3$. The $Pb_{(I)}S_8$ polyhedron shares one edge with the neighboring $Pb_{(II)}S_7$ polyhedra. These polyhedra extend parallel to the *c* axis, further sharing S atoms with their translation equivalents. The Pb and S atoms can be considered as forming a Pb_2S_6 layer. The $Pb_{(I)}S_8$ polyhedron shares an edge with an FeS_6 octahedron, and a $Pb_{(II)}S_7$ polyhedron shares a vertex with the FeS_6 octahedron. If a purely ionic viewpoint is adopted, the formula of jamesonite can be expressed as $Pb_4^{++}Fe^{++}(Sb_6S_{14})^{-10}$.

In the treatment of the crystal chemistry of sulfosalts[7] it is pointed out that the atomic aggregates of metallic, submetallic, and sulfur atoms found in sulfosalt structures can be derived from the various kinds of fragments of simpler sulfide structures, such as the galena

---

[15] E. HELLNER and G. LEINEWEBER, Über komplex zusammengesetzte sulfidische Erze: I. Zur Struktur des Bournonits, $PbCuSbS_3$, und Seligmannits, $PbCuAsS_3$. Z. Kristallogr. **107** (1956) 150—154.

type. Another way of looking at the Sb_6S_{14} group is, therefore, to regard it as one of the basic structural units. This group is, to first approximation, a small fragment of an octahedral layer sharing edges with four neighboring octahedra. Since the regular octahedral arrangement of six sulfur atoms around an Sb atom is not stable, this hypothetical fragment must be rearranged in some way. This is done to satisfy the requirements of the bonding nature of the Sb atoms. In jamesonite each Sb atom has three closest S atoms and four additional ones to form an SbS_7 coordination polyhedron. This type of coordination was observed for the Sb atoms in stibnite[16] and livingstonite[6], and also in Sb_I in berthierite[5]. For the Sb_{II} atoms in berthierite the number of additional atoms is three, and six S atoms surround the Sb atom in a distorted octahedral arrangement. These arrangements of additional S atoms seem to be influenced by the existence of the other kinds of metallic atoms in the structures.

The cleavage of jamesonite is reported as (1), basal cleavage which is good rather than perfect, and (2), prism zone cleavages (010), and (120). These cleavages can be explained as the result of the structural nature described above. The cleavage (120) occurs because of the breaking of the weaker bonds between two Sb_3S_7 groups. These bonds are indicated by dotted lines in Fig. 19. For cleavage parallel to (010), breaking of one bond of length 2.7 Å is necessary, but this bond density is smaller than in any other direction. As discussed above, the Sb—S distances between groups related by translation, *c* is about 3.0 Å, and the two shortest Fe—S distances are parallel to (001). The basal cleavage reported as good is understandable from these facts.

In summary, in the crystal structure of jamesonite, the basic structural principles found among the members of acicular sulfosalts are still observable. But the strongly bonded Sb—S layers or chains running parallel to the acicular axis are not well defined in jamesonite. Although that kind of atomic group can be discerned along the *c* axis, the strongest Sb—S bonds are oriented parallel to the (001) plane. The absence of these strongly bonded layers causes the tendency toward basal cleavage.

This research was supported by a grant from the National Science Foundation.

Crystallographic Laboratory, Massachusetts Institute of Technology,
Cambridge, Massachusetts, U.S.A.

[16] W. Hofmann, Die Struktur der Minerale der Antimonitgruppe. Z. Kristallogr. **86** (1933) 225—245.